Available online at www.sciencedirect.com
SCIENCE DIRECT®
Applied Geochemistry 19 (2004) 1655–1686
Applied Geochemistry
www.elsevier.com/locate/apgeochem

Geochemistry, radiocarbon ages, and paleorecharge conditions along a transect in the central High Plains aquifer, southwestern Kansas, USA

P.B. McMahon[a,*], J.K. Böhlke[b], S.C. Christenson[c]

[a] US Geological Survey, Denver Federal Center, Mail Stop 415, Denver, CO 80225, USA
[b] US Geological Survey, 431 National Center, 12201 Sunrise Valley Dr., Reston, VA 20192, USA
[c] US Geological Survey, 202 NW 66th, Bldg. 7, Oklahoma City, OK 73116, USA

Received 7 February 2003; accepted 10 May 2004
Editorial handling by Y. Kharaka

Abstract

Water samples from short-screen monitoring wells installed along a 90-km transect in southwestern Kansas were analyzed for major ions, trace elements, isotopes (H, B, C, N, O, S, Sr), and dissolved gases (He, Ne, N_2, Ar, O_2, CH_4) to evaluate the geochemistry, radiocarbon ages, and paleorecharge conditions in the unconfined central High Plains aquifer. The primary reactions controlling water chemistry were dedolomitization, cation exchange, feldspar weathering, and O_2 reduction and denitrification. Radiocarbon ages adjusted for C mass transfers ranged from <2.6 ka (^{14}C) B.P. near the water table to 12.8 ± 0.9 ka (^{14}C) B.P. at the base of the aquifer, indicating the unconfined central High Plains aquifer contained a stratified sequence of ground water spanning Holocene time. A cross-sectional model of steady-state ground-water flow, calibrated using radiocarbon ages, is consistent with recharge rates ranging from 0.8 mm/a in areas overlain by loess to 8 mm/a in areas overlain by dune sand. Paleorecharge temperatures ranged from an average of 15.2 ± 0.7 °C for the most recently recharged waters to 11.6 ± 0.4 °C for the oldest waters. The temperature difference between Early and Late Holocene recharge was estimated to be 2.4 ± 0.7 °C, after taking into account variable recharge elevations. Nitrogen isotope data indicate NO_3 in paleorecharge (average concentration = 193 μM) was derived from a relatively uniform source such as soil N, whereas NO_3 in recent recharge (average concentration = 885 μM) contained N from varying proportions of fertilizer, manure, and soil N. Deep water samples contained components of N_2 derived from atmospheric, denitrification, and deep natural gas sources. Denitrification rates in the aquifer were slow ($5 \pm 2 \times 10^{-3}$ μmol N L^{-1} a^{-1}), indicating this process would require >10 ka to reduce the average NO_3 concentration in recent recharge to the Holocene background concentration.
Published by Elsevier Ltd.

1. Introduction

The study of paleo ground waters with ages spanning Late Pleistocene and Holocene time has been used to better understand paleoclimate changes (Andrews and Lee, 1979; Stute et al., 1992; Aeschbach-Hertig et al., 2002), temporal variability in the amount and composition of ground-water recharge (Dutton, 1995; Edmunds and Smedley, 2000), and biogeochemical processes that may occur at extremely slow rates, like denitrification in generally oxic environments (Vogel et al., 1981). A primary requirement for extracting paleorecharge records from aquifers is the preservation of a sequence of ground-water ages along flow paths. Most records of recharge spanning Late Pleistocene and Holocene time

* Corresponding author. Fax: +1-303-236-4912.
E-mail address: pmcmahon@usgs.gov (P.B. McMahon).

0883-2927/$ - see front matter. Published by Elsevier Ltd.
doi:10.1016/j.apgeochem.2004.05.003

have been extracted from confined aquifers (Phillips et al., 1986; Stute and Schlosser, 1993; Plummer, 1993; Darling et al., 1997; Plummer and Sprinkle, 2001). Results from this study demonstrate that the unconfined central High Plains aquifer contains a stratified sequence of ground water recharged throughout Holocene time, modified locally by recent anthropogenic physical and chemical disturbances. The presence of paleorecharge in the High Plains aquifer, which produces about 28% of the ground water used for irrigation in the United States (Solley et al., 1993; McGuire and Sharpe, 1997), indicates the non-renewable nature of this heavily used resource.

This paper describes the geochemistry and water stratification based on radiocarbon ages along a transect in the central High Plains aquifer. Geochemical and isotopic data and radiocarbon ages are used to reconstruct records of temperature, NO_3 concentrations, and $\delta\,^{15}N[NO_3]$ and $\delta\,^{18}O[H_2O]$ values in paleorecharge. These paleorecharge records provide a baseline against which current recharge conditions are compared. Nitrate concentrations in recent recharge are evaluated relative to denitrification rates calculated for this largely oxic aquifer.

2. Hydrologeologic setting

The study area for this investigation consisted of a transect along presumed ground-water flow paths in the central High Plains aquifer in southwestern Kansas (Fig. 1). The 126,000-km^2 central High Plains aquifer consists of the Ogallala Formation and any saturated material of Quaternary age hydraulically connected to the Ogallala Formation (Luckey and Becker, 1999). The Tertiary Ogallala Formation consists primarily of unconsolidated clay, silt, sand, and gravel with scattered cemented zones consisting of $CaCO_3$. Reworked sediments of Permian age containing dolomite and anhydrite/gypsum are present in basal sands and gravels in the aquifer (Smith, 1940). The upper surface of the Ogallala Formation has been reworked by fluvial and eolian erosion and deposition during the Quaternary Period. These deposits consist of gravel, sand, silt, and clay where fluvial erosion and deposition have reworked the Ogallala Formation, and loess and dune sand where eolian processes have dominated (Gutentag et al., 1984).

In southwestern Kansas, the pre-Ogallala surface consists of consolidated rocks of Late Permian to Late Cretaceous age (Gutentag et al., 1981). At the western end of the transect, rocks of the pre-Ogallala surface are of Late Triassic, Late Jurassic, and Early Cretaceous age (Fig. 1), primarily of the Dockum Group and Morrison Formation (Gutentag et al., 1981; Whittemore et al., 1993). These sediments consist of shale, sandstone, limestone, dolomite, and conglomerate (Gutentag et al., 1984). Along the central and eastern parts of the transect, the geologic units underlying and in contact with the Ogallala Formation are Permian-age rocks, including the Whitehorse Group, Big Basin Formation, and the Day Creek Dolomite (Gutentag et al., 1981). These rocks consist of shale, siltstone, sandstone, anhydrite, gypsum, dolomite, and limestone. The Permian Blaine Formation and Flowerpot Shale underlie the Ogallala Formation but are not in direct contact with it. Dissolution of bedded halite in the Flowerpot Shale resulted in the formation of filled collapse basins and the Crooked Creek Fault at the eastern end of the transect (Gustavson et al., 1980).

Ground water in the High Plains aquifer generally responds to changes in storage as an unconfined aquifer, although local confinement from less permeable geologic units has been observed (Gutentag et al., 1984; McMahon, 2001). At a regional scale, the potentiometric surface slopes from west to east (Fig. 1) with a hydraulic gradient of about 2 m/km (Gutentag et al., 1981). Saturated thickness gradually increases along the transect from near zero at the western end to a maximum of about 175 m near the center of the transect, then gradually decreases to about 70 m at the eastern end of the transect on Crooked Creek (Figs. 1 and 2). A short distance east of Crooked Creek the Ogallala Formation has been removed by erosion.

Recharge to the High Plains aquifer is from infiltration of precipitation through the soil zone (diffuse recharge), infiltration of surface water through streambeds (stream infiltration), and infiltration of irrigation water. The rate of recharge to the High Plains aquifer has been the subject of many studies and was investigated by Theis as early as 1937 (Theis, 1937). A summary of many recharge estimates, ranging from 1.5 to 150 mm/a, with a median recharge of 19 mm/a, was presented in Gutentag et al. (1984). These estimates were largely based on water-budget methods or model simulations of ground-water movement, and did not include evidence from ground-water age-depth relations. Meyer et al. (1970) estimated recharge to the High Plains aquifer in Finney County, Kansas (north of the transect) at 36 mm/a during a period of above-normal precipitation. For the same area they estimated recharge at 1 mm/a for the long-term average using ground-water levels to calculate the change in water in storage and a mass-balance calculation to determine recharge.

Streams provide recharge to and serve as discharge zones for ground water. Gutentag et al. (1984) noted that ephemeral streams contribute large amounts of recharge during their rare periods of significant flow. The Cimarron River is of particular interest to this study because the Cimarron River is assumed to be a discharge area along the eastern end of the transect. Based on an analysis of long-term stream discharge records, Luckey and Becker (1998) indicated the High Plains aquifer discharged about 8.84 m^3/s to the Cimarron River before the development of large volumes of irrigation

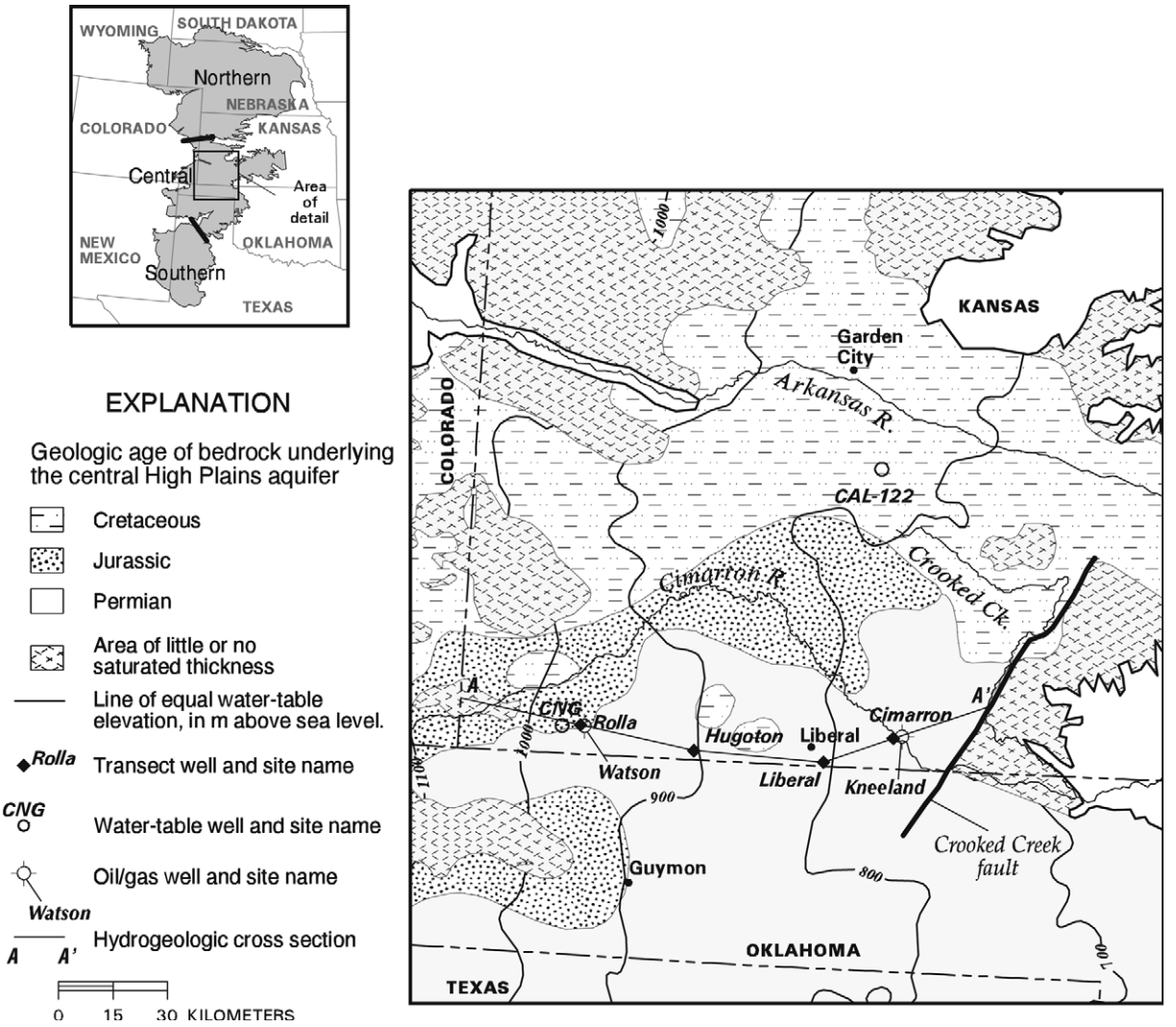

Fig. 1. Location of the study area in the High Plains aquifer area, geologic age of bedrock underlying the aquifer, and March 2000 water-table elevations in the aquifer. Hydrogeologic cross-section A–A′ is shown in Fig. 2. Bedrock geology from Gutentag et al. (1984) and water-table elevation data from G. McGuire (US Geological Survey, written communication, 2001).

withdrawals from the aquifer, and that discharge has decreased substantially in response to those withdrawals. Crooked Creek, at the eastern end of the transect, also is a discharge area for ground water in the High Plains aquifer. Numerous springs are located in the valley of Crooked Creek that discharge water from the High Plains aquifer.

3. Methods

3.1. Site selection and installation of transect wells

Predevelopment and 1999 potentiometric-surface maps were initially consulted to select transect well sites along ground-water flow paths through the thickest section of the central High Plains aquifer (Cederstrand and Becker, 1999). At the scale of this study, directions of ground-water movement indicated by the predevelopment and 1999 maps were the same. Output from an existing MODFLOW model of ground-water movement in the study area (Luckey and Becker, 1999) was used as input in MODPATH (Pollock, 1994), the USGS particle-tracking model designed to work with MODFLOW, to verify that the selected well locations were aligned along flow paths. The existing model was run under steady-state conditions and calibrated to predevelopment heads.

After the sites for the transect wells were selected, wells were installed using a mud-rotary drill rig at the 4

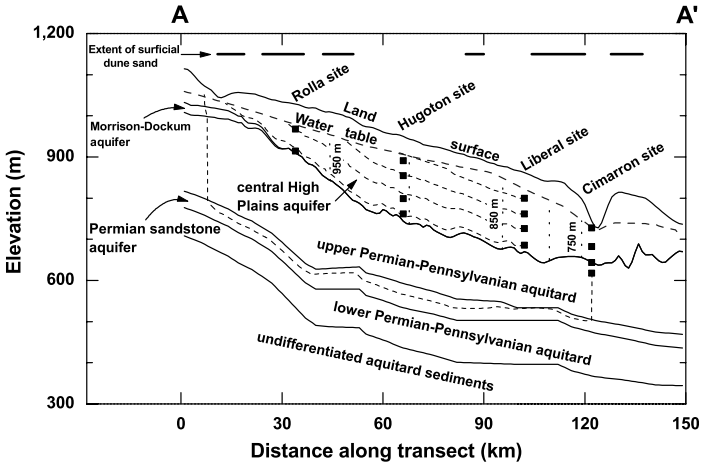

Fig. 2. Hydrogeologic cross-section A–A′ showing elevations of transect well screens (solid squares), ground-water-elevation contours based on March 2000 measurements, and simulated flow paths (small dashed lines) to the Liberal and Cimarron-436 wells. Extent of surficial dune sand from Kansas Geological Survey. Hydrogeologic names for the Permian units and top elevations for the Lower Permian-Pennsylvanian aquitard and Permian sandstone aquifer adapted from Macfarlane et al. (1993). Base of the central High Plains aquifer derived from water-well drillers' logs and boreholes drilled for this study.

transect well sites, and a casing-advance system with air return flow was used at the two water-table well sites (Fig. 1). Wells were installed from April through mid June, 1999. Well construction details are listed in Table 1.

3.2. Sediment sample collection

Sediment cuttings and cores were collected at selected depths from the transect boreholes for semiquantitative X-ray diffraction (XRD) analysis, inorganic and organic C analyses, and analyses of $\delta\ ^{13}C$[carbonate], $\delta\ ^{18}O$[carbonate], $\delta\ ^{34}S$[anhydrite/gypsum] (hereinafter referred to as $\delta\ ^{34}S[CaSO_4]$), $^{87}Sr/^{86}Sr[CaSO_4]$, and $^{87}Sr/^{86}Sr$[dolomite]. The Cimarron borehole was the only one to penetrate the Permian-Pennsylvanian aquitard (Fig. 2); therefore, additional samples of the aquitard were obtained from the cuttings repository of the Kansas Geological Survey in Wichita, KS. Cuttings from oil/

Table 1
Well construction details

Well name	Elevation of land surface (m)	Depth to base of central High Plains aquifer (m)	Depth to water at time of construction (m)	Total depth of well (m)	Open interval (m)
Central High Plains aquifer					
CAL-122	863	–	45.2	47	43–46
CNG	1036	–	50.0	59	53–56
Rolla-193	1024	122	54.6	60	53–59
Rolla-366	1024	122	54.6	113	109–112
Hugoton-140	948	194	38.4	44	37–43
Hugoton-313	948	194	38.7	97	92–95
Hugoton-495	948	194	38.4	152	148–151
Hugoton-617	948	194	39.0	191	185–188
Liberal-160	858	176	36.3	50	43–49
Liberal-319	858	176	42.1	99	94–97
Liberal-436	858	176	42.1	134	130–133
Liberal-570	858	176	41.8	177	171–174
Cimarron-65	745	105	17.7	21	14–20
Cimarron-210	745	105	16.2	66	61–64
Cimarron-336	745	105	17.1	104	99–102
Upper Permian-Pennsylvanian aquitard					
Cimarron-436	745	–	17.1	134	121–133

gas wells drilled near the Rolla and Cimarron sites were used (Watson and Kneeland sites in Fig. 1). Sediment cores collected from the unsaturated zones at the CNG and CAL-122 sites were analyzed for $\delta\ ^{15}N[NO_3]$.

3.3. Sediment sample analysis

Sediment samples for XRD analysis were oven dried at 50 °C for 24 h, sieved to remove the >2-mm fraction, ground into a powder, and mounted onto slides for analysis with no further treatment. Total and carbonate C were analyzed according to ASTM methods (American Society For Testing And Materials, 1992, 1993). Organic C was determined as the difference between total C and inorganic C. The detection limits for inorganic and organic C were 0.02 and 0.05 wt%, respectively.

Carbon, O, S and Sr isotope analyses were performed on minerals manually separated from the bulk sediment by inspection with a binocular microscope. Mineralogy of the separates was verified by XRD analysis. For mineral separates containing calcite and dolomite, $\delta\ ^{13}C$ and $\delta\ ^{18}O$ values for both minerals were analyzed according to the timed phosphoric-acid-dissolution procedure of Walters et al. (1972). For mineral separates containing anhydrite/gypsum and dolomite, extraction of Sr from both minerals for $^{87}Sr/^{86}Sr$ analysis was performed using cold (9 °C) 0.2 N HCl for dolomite (1-h extraction) followed by warm (25 °C) 2 N HCl for anhydrite/gypsum (24-h extraction). Analyses of C, O, and S isotopes were performed at the USGS Stable Isotope Laboratory in Denver, Colo, and reported relative to VPDB, VSMOW, and VCDT, respectively. Analyses of Sr isotopes were performed at the USGS Thermal-Ionization Mass Spectrometry Laboratory in Menlo Park, CA.

Nitrogen isotope analyses were performed on NO_3 extracted from unsaturated-zone cores using a modification of the extraction procedures of Lindau and Spalding (1984) and Herbel and Spalding (1993). Nitrate was extracted from sediment by combining 10 g of oven-dried (50 °C) sediment (<2 mm) with 100 mL of deionized water in plastic beakers, mixing on an orbital shaker at 170 rpm for 1 h, and filtering the solution through 0.45-μm syringe filters. At each sampling depth, additional aliquots of sediment were extracted until sufficient N mass (>10 μmol) was obtained for N isotope analysis. Nitrogen isotope analyses were performed as described below for dissolved NO_3.

3.4. Water sample collection

The wells were developed on three separate dates in June, July, and August, 1999 prior to sampling to ensure water representative of the aquifer was collected for this study. Protocols used to measure water temperature, specific conductance, pH, and O_2 in the field and to collect ground-water samples were described in detail in Koterba et al. (1995).

Water samples collected for analyses of major ions, alkalinity, trace elements, nutrients, $\delta\ ^{11}B$, $\delta\ ^{15}N[NO_3]$, $\delta\ ^{34}S[SO_4]$, and $^{87}Sr/^{86}Sr$ were filtered in the field using a 0.45-μm disposable capsule filter and collected in polyethylene bottles that were rinsed with filtered ground water. The major cation and trace element samples were acidified in the field to a pH < 2 using ultrapure HNO_3. The $^{87}Sr/^{86}Sr$ samples were acidified in the laboratory. The major anion, nutrient, $\delta\ ^{15}N[NO_3]$, and $\delta\ ^{34}S[SO_4]$ samples were stored on ice with no further preservation. Samples for $\delta\ ^{15}N[NO_3]$ analysis were then frozen within a few days. Alkalinity was determined in the field by incremental titration of the filtered water sample using 1.6 N H_2SO_4.

Samples for the analysis of C isotopes in dissolved inorganic C ($\delta\ ^{13}C$[DIC] and ^{14}C) were collected in 250-mL glass bottles that were sealed with plastic screw caps fitted with Teflon-coated septa. The bottles were filled from the bottom and allowed to overflow for 5 min prior to creating a 2-mL air headspace in the bottles and the caps were sealed with electrical tape. The C isotope samples were not filtered unless the ground water contained visible suspended material. The samples were stored on ice with no further preservation.

Water samples collected for the analysis of dissolved organic C (DOC) were filtered in the field through 0.45-μm Ag filters, collected in amber glass bottles, and stored on ice with no further preservation.

Unfiltered ground water was collected for analyses of ^{3}H, $\delta\ ^{18}O[H_2O]$, $\delta\ ^{2}H[H_2O]$, $\delta\ ^{15}N[N_2]$, $\delta\ ^{3}He$, and concentrations of the dissolved gases He, N_2, Ne, Ar, O_2, and CH_4. Tritium samples were collected in 1-L high density polyethylene bottles with screw caps that were secured with electrical tape. Samples for $\delta\ ^{18}O[H_2O]$ and $\delta\ ^{2}H[H_2O]$ analyses were collected in 40-mL glass bottles with screw caps that were secured with electrical tape. Samples for analyses of $\delta\ ^{15}N[N_2]$, N_2, Ar, O_2, and CH_4 were collected in 125-mL serum bottles that were sealed with thick rubber stoppers (Bellco Glass, Inc., Vineland, NJ). The bottles were filled from the bottom and allowed to overflow for 5 min in a bucket of water to ensure no air bubbles were trapped inside. Pellets of KOH were added to the sample to raise pH > 11 and inhibit microbial activity. The bottles were sealed with no headspace and stored on ice. Samples for He and Ne analyses were collected using the techniques described by Castro et al. (2000).

3.5. Water sample analysis

Major ion, trace element, nutrient, and DOC samples were analyzed at the US Geological Survey National Water Quality Laboratory using the techniques

described by Fishman and Friedman (1989) and Wershaw et al. (1987). The average charge balance of analyses (calculated relative to the sum of the equivalents of cations and anions) is $1.2 \pm 0.9\%$. Dissolved N_2, Ar, O_2, and CH_4 were measured by gas chromatography with thermal conductivity or flame ionization detection at the USGS Chlorofluorocarbon Laboratory in Reston, VA (Busenberg et al., 1993; http://water.usgs.gov/lab/dissolved-gas/). Precision of these analyses was better than ± 2 %.

Measurements of δ $^{2}H[H_2O]$, δ $^{18}O[H_2O]$, and δ $^{34}S[SO_4]$ were performed at the USGS Stable Isotope Laboratory in Reston, VA. Hydrogen and O isotopic analyses were performed using the techniques of Coplen et al. (1991) and Epstein and Mayeda (1953). Results are reported in per mil (‰) relative to VSMOW, normalized to VSMOW of SLAP (Coplen, 1988). The 2-σ uncertainties of H and O isotopic results are 2 and 0.2‰, respectively. Dissolved SO_4 samples were collected and prepared for isotopic analysis using the methods of Carmody et al. (1997). Sulfur isotope ratios are reported in per mil relative to VCDT. The 2-σ uncertainty of S isotopic results is 0.4‰.

Measurements of δ ^{3}He and concentrations of He and Ne were performed at the Lamont-Doherty Earth Observatory, Noble Gas Laboratory in Palisades, NY (Ludin et al., 1998). Measurements of δ $^{13}C[DIC]$, reported relative to VPDB, and ^{14}C sample preparation were performed at the University of Waterloo in Ontario, Canada. Measurements of ^{14}C were performed at the IsoTrace Radiocarbon Laboratory AMS facility in Toronto, Canada, using accelerator mass spectrometry. Reported ^{14}C values (in percent modern C, pmc) are not adjusted for the difference between −25‰ and the δ ^{13}C value of the sample.

Strontium and B isotope analyses were performed at the USGS Thermal-Ionization Mass Spectrometry Laboratory in Menlo Park, CA. Ratios of $^{87}Sr/^{86}Sr$ were analyzed by the positive ion thermal mass spectrometry method with a precision of 0.00002. Boron isotopes were analyzed by the negative ion thermal mass spectrometry method with a δ ^{11}B precision of ±0.5‰ and reported relative to NIST 951 H_3BO_3.

Measurements of δ $^{15}N[NO_3]$ and δ $^{15}N[N_2]$ were made using modifications of the methods described by Böhlke and Denver (1995) and Böhlke et al. (2002). δ $^{15}N[NO_3]$ values are reported with respect to atmospheric N_2 and were calibrated by analyses of aqueous NO_3 laboratory standards prepared as samples and normalized to values of +0.4 and +180.0‰ for IAEA-N1 and USGS-32, respectively (Böhlke and Coplen, 1995). Values of δ $^{15}N[N_2]$ were calibrated by analyses of air (0‰), and the procedures were verified by analyses of air-saturated water samples that were collected at 16 °C under controlled laboratory conditions, prepared as samples, and yielded δ $^{15}N[N_2]$ values equal to $+0.72 \pm 0.03$‰ consistent with air–water equilibrium (Klots and Benson, 1963; Hübner, 1986). The O isotopic composition of NO_3 was measured in samples from two profiles (Liberal and Cimarron). This was done by reducing the NO_3 to N_2O using a bacterial culture, followed by continuous-flow mass spectrometry on the N_2O, as described by Casciotti et al. (2002). The δ $^{18}O[NO_3]$ analyses were calibrated by analyzing aliquots of reference materials USGS-34 and IAEA-N3, for which δ ^{18}O values were assumed to be −27.9*permil* and +25.6*permil*, respectively, with respect to VSMOW (Böhlke et al., 2003). Reference materials and samples had reproducibilities averaging ±0.2–0.3‰. The corresponding δ $^{15}N[NO_3]$ values determined by the bacterial N_2O method (Sigman et al., 2001) were not significantly different from the values measured in combusted samples (Table 4).

Tritium in water was measured at the USGS Tritium Laboratory (Menlo Park, CA) by electrolytic concentration and liquid scintillation counting. The minimum reporting level was 0.3 TU, and the average 2-σ precision of the analyses was 0.3 TU.

3.6. Ground-water flow modeling

A ground-water flow model was constructed using MODFLOW-96 (Harbaugh and McDonald, 1996). Particle-tracking analysis was performed using MODPATH (Pollock, 1994). MODFLOW and MODPATH were run with the Department of Defense Groundwater Modeling System (GMS) software (Boss International, 1997).

The flow model was constructed to follow the presumed flow paths through each of the 4 transect well sites (Fig. 1). The physical boundaries incorporated in the model (the altitude of land surface, water table, and base of the High Plains aquifer) were defined by intersecting the transect path with mathematical surfaces defined by interpolating from control-point wells near the flow path. The model was a two-dimensional vertical slice in concept, but MODFLOW and MODPATH require some width (*Y*-dimension), which was arbitrarily set to 1000 m. The model contained 149 columns and 10 layers in the *X*- and *Z*-dimensions, respectively. All cells were 1000 m in the *X*-dimension, but the cell thicknesses (*Z*-dimension) were variable. Because vertical ground-water flow is significant to this investigation, the High Plains aquifer and underlying bedrock formations were each divided into 5 layers, for a total of 10 layers. The High Plains aquifer was subdivided into layers by computing the total saturated thickness of the aquifer at each cell and dividing the model into 5 layers of equal saturated thickness. The topmost layer includes the unsaturated zone, so the topmost layer is thicker than the other 4 layers representing the High Plains aquifer. The base of the model was somewhat arbitrarily set to sea

Table 2
Values of horizontal hydraulic conductivity assigned to model layers

Model layer	Hydrostratigraphic unit	Horizontal hydraulic conductivity (m/d)
1–5	Central High Plains aquifer	0.1–2.88
6	Morrison-Dockum aquifer	0.045
7	Upper Permian-Pennsylvanian aquitard	8.2×10^{-4}
8	Permian sandstone aquifer (Cedar Hills Sandstone)	0.18
9	Lower Permian-Pennsylvanian aquitard	8.2×10^{-4}
10	undifferentiated aquitard sediments	8.2×10^{-4}

Data from Whittemore et al. (1993).

level. The bedrock underlying the High Plains aquifer was subdivided into 5 layers (Fig. 2). Hydraulic conductivity for each of these layers was taken from Whittemore et al. (1993) (Table 2). Whittemore et al. (1993) assumed that vertical hydraulic conductivity was one order of magnitude less than horizontal hydraulic conductivity, and that assumption was also used in the High Plains transect model.

The Cimarron River crosses the transect at two points, near the western end of the transect and near the eastern end of the transect (Fig. 1). The river was simulated as a constant head cell in the uppermost layer of the model. Constant head cells allow ground water to recharge or discharge the flow system, depending on the gradients in the adjacent cells. Crooked Creek was also simulated as a constant head cell at the eastern end of the transect.

The flow model was initially calibrated by applying the median recharge rate of 19 mm/a from the summary in Gutentag et al. (1984) to the cells in the model representing the land surface and adjusting hydraulic conductivity to match the 1980 measured heads. Hydraulic-conductivity adjustments were made using the optimization package in the GMS software. The model was run assuming conditions in the simulated part of the aquifer were at a steady-state condition. The entire High Plains aquifer has been developed to some degree by wells withdrawing ground water, but the area simulated by the flow model is relatively lightly developed, and heads measured in 1980 were generally less than 3 m below the predevelopment heads (Luckey et al., 1986).

After a reasonable match between simulated head and 1980 measured head was achieved, a MODPATH particle-tracking analysis was initiated. MODPATH uses the results of the MODFLOW-96 simulation and determines paths and travel times of ground-water movement. In addition to the MODFLOW-96 simulation, MODPATH requires porosity, which was set to 0.33 in the High Plains aquifer and 0.11 in the underlying bedrock (Jones and Schneider, 1969; Jorgensen et al., 1993; McMahon et al., 2003). In the model, hypothetical "particles" of water were placed at locations corresponding to the top, center, and bottom of the well screens in the 4 transect well clusters and tracked backwards in the ground-water flow field to their recharge locations. The travel times for the particles were compared to the radiocarbon age for water samples from that well. Other calibration procedures used to optimize the match between particle and radiocarbon ages are discussed later in this paper.

4. Results and discussion

4.1. Ground-water chemistry

Changes in the chemical and isotopic compositions of ground water along flow paths, knowledge of the mineral phases present in the aquifer, and mineral saturation indices (SI) can be used to infer possible geochemical reactions occurring in the aquifer. Water from wells Rolla-193, CNG, Hugoton-140, and Cimarron-65 were assumed to be representative of recharge in the transect area because those wells were screened within 3 m of the water table (Table 1). The other transect wells were screened farther below the water table; thus, they were considered to be located downgradient from the water table. The composition of recharge water varied from Ca–HCO_3 (CNG) to Ca–Na–HCO_3 (Rolla-193 and Cimarron-65) to Na-HCO_3 (Hugoton-140) type. The water composition evolved to distinctly different types at the base of the aquifer: Ca–SO_4 type at the Rolla site, Ca–HCO_3 type at the Hugoton site, Ca–Mg–HCO_3 type at the Liberal site, and Na–Cl type at the Cimarron site. Concentrations of Ca and Mg increased and concentrations of DIC decreased with increasing SO_4 concentrations (Table 3 and Figs. 3(a) and (b)). Chloride concentrations increased with depth in the aquifer (Table 3), which can be accounted for by mixing small percentages of halite-dissolution brine from the Permian-Pennsylvanian aquitard with water from the aquifer (Fig. 3(c)). The increases in concentrations of Ca, Mg, and SO_4 and decrease in DIC concentrations cannot be explained solely by mixing between these two waters.

Concentration trends similar to those in the central High Plains aquifer were described in the Madison aquifer in Montana and South Dakota and were

Table 3
Physical properties and concentrations of major ions, nutrients, and trace elements in water from sampled wells in the central High Plains aquifer and Upper Permian-Pennsylvanian aquitard

Well name	Sample date	Depth of screen top below water table (m)	pH	Temperature (°C)	O_2	DIC	DOC	Ca	Mg	Na	K	Cl
Central High Plains aquifer												
CAL-122	7/10/00	−2.6	7.43	17.3	19	3120	212	3140	910	1200	170	370
CNG	7/25/00	2.8	7.50	19.9	>220	3380	25	1550	520	1040	50	320
Rolla-193	8/30/99	−1.5	7.70	22.7	262	3600	–	1070	270	1850	110	300
Rolla-366	8/30/99	54	7.47	19.7	180	3060	42	3320	1710	2080	90	440
Hugoton-140	8/29/99	−3.5	7.65	23.8	–	4280	133	980	480	3230	210	600
Hugoton-313	8/29/99	45	7.50	19.1	192	3170	125	1760	880	860	90	340
Hugoton-495	8/28/99	95	7.66	20.5	173	3370	25	1590	780	860	80	340
Hugoton-617	8/28/99	131	7.64	20.5	191	3330	33	1670	790	880	80	360
Liberal-160	8/27/99	7.3	7.65	23.6	205	4320	42	960	1420	780	90	560
Liberal-319	8/27/00	49	7.72	18.5	108	3600	33	1100	980	1100	90	260
Liberal-436	8/26/99	85	7.59	21.7	100	3390	33	1040	930	1150	100	280
Liberal-570	8/26/99	126	7.47	19.9	53	3880	42	1170	990	1570	100	360
Cimarron-65	9/1/99	−3.1	7.59	18.1	216	3300	33	1360	580	2120	120	2010
Cimarron-210	8/31/99	45	7.50	18.6	221	3450	25	1670	770	1820	90	1480
Cimarron-336	9/1/99	83	7.13	19.0	63	3260	25	7490	6090	33,100	270	52,500
Upper Permian-Pennsylvanian aquitard												
Cimarron-436	8/31/99	104	7.15	20.0	17	1920	<8	19,400	17,700	167,000	450	215,000
	10/18/00	105	7.30	19.6	10	1950	–	18,700	17,700	176,000	510	220,000

Well name	SO_4	Br	SiO_2	NH_4 + Org N	NH_4	NO_2 + NO_3	NO_2	Al	B	Fe	Mn	Sr
Central High Plains aquifer												
CAL-122	2830	2.9	180	7	<1.4	18	0.9	<0.04	–	<0.18	14	–
CNG	730	1.4	450	<7	<1.4	87	<0.7	<0.04	–	<0.18	1.1	–
Rolla-193	240	0.9	490	18	18	408	<0.7	0.04	4.2	<0.18	0.44	4.3
Rolla-366	4500	1.9	500	<7	<1.4	171	9.1	0.04	14.7	<0.18	<0.05	23.6
Hugoton-140	630	1.6	570	76	76	160	2.5	<0.04	9.2	<0.18	0.12	7.4
Hugoton-313	1270	1.7	530	<7	<1.4	183	<0.7	0.05	6.7	<0.18	<0.05	12.4
Hugoton-495	1090	1.7	500	<7	<1.4	179	<0.7	<0.04	5.9	<0.18	<0.05	11.1
Hugoton-617	1220	1.7	510	<7	<1.4	164	<0.7	<0.04	6.1	<0.18	<0.05	10.9
Liberal-160	220	1.2	900	<7	<1.4	136	<0.7	<0.04	6.6	<0.18	<0.05	16.8

Liberal-319	640	1.3	520	7	<1.4	225	<0.7	0.05	7.6	<0.18	<0.05	17.0
Liberal-436	620	1.3	480	<7	<1.4	219	<0.7	<0.04	6.9	<0.18	<0.05	15.2
Liberal-570	910	1.2	460	<7	<1.4	169	<0.7	<0.04	10.1	<0.18	0.14	19.4
Cimarron-65	380	1.0	380	16	13	148	0.9	<0.04	6.3	<0.18	0.09	8.0
Cimarron-210	800	1.7	450	7	<1.4	219	<0.7	<0.04	8.7	<0.18	<0.05	11.2
Cimarron-336	2720	5.3	450	7	<1.4	164	<0.7	<0.11	18.8	<0.90	2.4	104
Upper Permian-Pennsylvanian aquitard												
Cimarron-436	13,200	3.3	640	<7	<1.4	28	<0.7	<0.37	56.8	<3.6	2.0	–
	13,300	17	600	<7	3.3	23	<0.7	<0.37	56.6	<2.1	1.2	341

Concentrations in micromoles per liter.

attributed to dedolomitization reactions (i.e., dolomite dissolution and calcite precipitation driven by gypsum or anhydrite dissolution) (Back et al., 1983; Plummer et al., 1990; Busby et al., 1991). The Madison aquifer is composed of a massive carbonate sequence; however, dedolomitization reactions also have been proposed in the Midlands Triassic sandstone aquifer in England (Edmunds and Smedley, 2000). All but 3 of the High Plains water samples had calcite and dolomite saturation indices, SI, between ±0.25 (Fig. 3(d)), indicating they were essentially in equilibrium with respect to those mineral phases (Plummer et al., 1990; Parkhurst et al., 1992). Thus, those minerals were not likely to dissolve further in the absence of other chemical changes. All of the water samples were undersaturated with respect to anhydrite (and gypsum), indicating those SO_4 minerals had the potential to dissolve. Anhydrite SI shifted closer to equilibrium as SO_4 concentrations increased along flow paths (Fig. 3(d)), suggesting that it was dissolving in the aquifer. During dedolomitization, anhydrite dissolution adds Ca to solution, thereby supersaturating the water with respect to calcite. In order for the water to remain in equilibrium with respect to calcite that mineral must then precipitate. During the process of calcite precipitation, DIC concentrations and pH values decrease, resulting in dolomite undersaturation and dissolution.

Recharge waters had the smallest SO_4 concentrations and $\delta\ ^{34}S[SO_4]$ values ranging from 0 to 3‰ (Fig. 4(a)). As that water moved downgradient, SO_4 concentrations increased and $\delta\ ^{34}S[SO_4]$ values approached values characteristic of anhydrite/gypsum in the Permian-Pennsylvanian aquitard (10.5–13‰). The $\delta\ ^{34}S[CaSO_4]$ values for Permian anhydrite/gypsum measured in this study are typical for Permian evaporites in the Kansas/Oklahoma area (Denison et al., 1998). These data indicate anhydrite/gypsum in the aquitard, or eroded from the aquitard and deposited in the Ogallala Formation, was an important source of SO_4 in the aquifer.

Krothe and Oliver (1982) identified an area of the aquifer between the Cimarron River and Crooked Creek Fault, NE of the study area (Fig. 1), in which $\delta\ ^{34}S[SO_4]$ values were negative, indicating a reduced S source for the SO_4. They proposed that H_2S from underlying formations migrated upward into the aquifer where it was oxidized to SO_4. In this study, H_2S was not detected in the underlying aquitard (Cimarron-436), and the $\delta\ ^{34}S$ value for SO_4 in the aquitard was about +10.8‰ (Table 4). It is possible the chemistry of water in the aquitard in the Krothe and Oliver (1982) study area differed from the chemistry in the present study area or that the source of SO_4 with negative $\delta\ ^{34}S$ values was not the underlying formations. CAL-122, located north of the transect area (Fig. 1), was screened just below the water table at the top of a 20-m-thick silty clay. That well produced a Ca–SO_4 type water with a $\delta\ ^{34}S[SO_4]$ value of −45‰. That δ

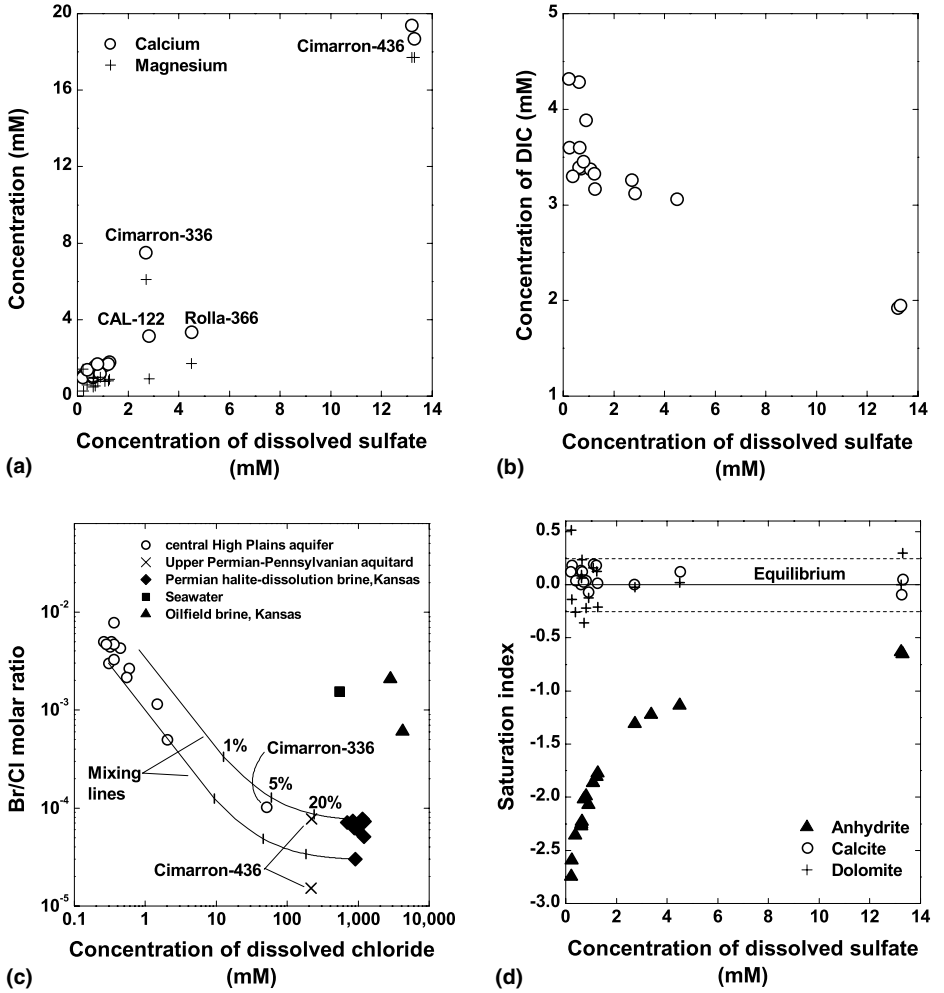

Fig. 3. (a) Concentrations of Ca and Mg versus SO_4 concentration, (b) concentration of DIC versus SO_4 concentration, (c) Br/Cl molar ratios versus chloride concentration, and (d) saturation indices for anhydrite, calcite, and dolomite versus sulfate concentration. Saturation indices were calculated using the WATEQFP speciation model in the computer program NETPATH (Plummer et al., 1994). The computer program PHRQPITZ (Plummer et al., 1988) was used to calculate saturation indices for water from Cimarron-436. The percentages in (c) refer to the amount of halite-dissolution brine in the mixture. Data for halite-dissolution brines in sediments of Permian age in south-central Kansas from Whittemore (1993) and data for seawater and oilfield brines in southwestern Kansas from Whittemore (1984).

$^{34}S[SO_4]$ value is indicative of reduced S that was later oxidized to produce dissolved SO_4. One possible source of the reduced S may be sediments eroded from Cretaceous marine shales located adjacent to the aquifer area in Colorado, Kansas, and New Mexico.

Variations in Sr concentrations and $^{87}Sr/^{86}Sr$ ratios in ground water are consistent with dissolution of anhydrite/gypsum and/or dolomite derived from the Permian-Pennsylvanian aquitard (Fig. 4(b)). With the increase in Sr concentrations along flow paths in the aquifer, $^{87}Sr/^{86}Sr$ ratios in dissolved Sr approached values measured in anhydrite/gypsum and dolomite from the aquitard. The range of $^{87}Sr/^{86}Sr$ ratios in the present anhydrite/gypsum samples (0.70744–0.70821) was similar to the range of $^{87}Sr/^{86}Sr$ ratios (0.70750–0.70932) measured in anhydrite/gypsum in the Permian Blaine Formation in western Oklahoma (Denison et al., 1998). Most of the $^{87}Sr/^{86}Sr$ ratios in the anhydrite/gypsum and dolomite samples were within the range of values reported for Permian seawater (Burke et al., 1982). However, the most radiogenic $^{87}Sr/^{86}Sr$ ratios (larger than about 0.70810) indicated the presence of a continentally derived Sr component in the minerals (Denison et al., 1998).

Several trends in the chemical and isotopic composition of High Plains ground water support the

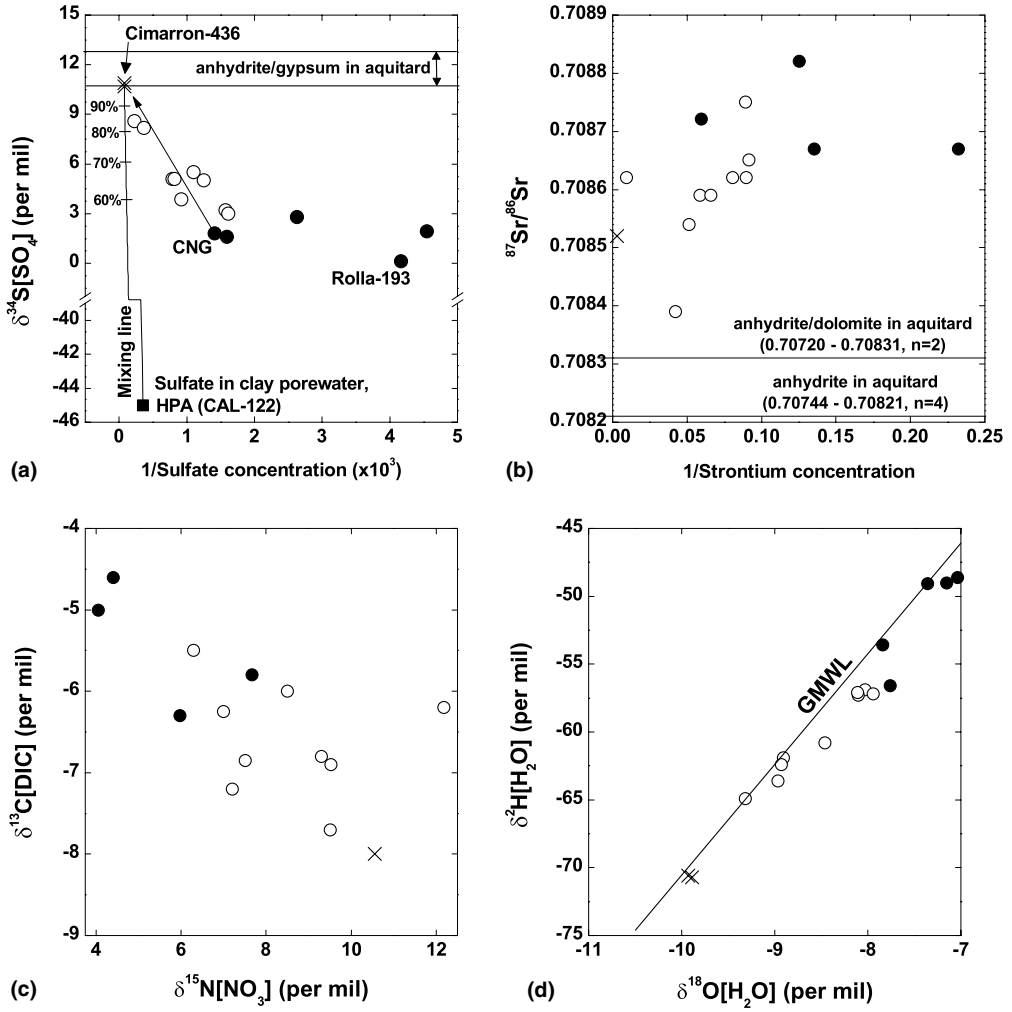

Fig. 4. (a) δ $^{34}S[SO_4]$ versus inverse SO_4 concentration. Percentages refer to mixtures of water from the Upper Permian-Pennsylvanian aquitard and clay in the High Plains aquifer. Arrow indicates possible pathway for the chemical evolution of recharge water along flow paths. (b), $^{87}Sr/^{86}Sr$ ratios versus inverse Sr concentration. (c), δ $^{13}C[DIC]$ versus δ $^{15}N[NO_3]$. (d), δ $^{2}H[H_2O]$ versus δ $^{18}O[H_2O]$. GMWL refers to the Global Meteoric Water Line (Craig, 1961). Solid circles represent samples collected near the water table in the aquifer, open circles represent samples collected downgradient from the water table in the aquifer, and crosses represent samples collected from the Upper Permian-Pennsylvanian aquitard.

hypothesis that dedolomitization was an important process controlling major-ion chemistry in the aquifer. Those trends include positive correlations between Ca, Mg and SO_4 concentrations, inverse correlation between DIC and SO_4 concentrations, mineral saturation indices, and the trends in δ $^{34}S[SO_4]$ and $^{87}Sr/^{86}Sr$ values toward values characteristic of anhydrite/gypsum and dolomite in the aquitard. The plausibility of dedolomitization occurring in the central High Plains aquifer, in light of constraints imposed by C isotope data and the availability of anhydrite and dolomite in the aquifer to dissolve, will be discussed later in this paper.

Oxygen was present in ground water throughout the aquifer; however, O_2 concentrations decreased with depth below the water table at 3 of the 4 transect sites (Table 3), indicating some O_2 reduction occurred in the aquifer. For example, O_2 concentrations decreased from 216 to 10 μM from the shallowest to deepest well at the Cimarron site. Decreases in O_2 concentrations with depth also were observed at the Rolla and Liberal sites. Vertical mixing of water in the aquifer at the Hugoton site during pumping of a nearby irrigation well probably accounts for the lack of a vertical gradient in O_2 concentrations at that site. Although data from 3 of the 4 transect sites indicated O_2 reduction occurred in the aquifer, only water from fine-grained deposits in the aquifer (CAL-122) and from the aquitard (Cimarron-436) had O_2 concentrations near 10 μM, considered to

Table 4
Isotope data for water and sediment from the central High Plains aquifer and Upper Permian-Pennsylvanian aquitard

Well name	Sample date	^{3}H (TU)	$\delta\ ^{2}H[H_2O]$ (‰)	$\delta\ ^{18}O[H_2O]$ (‰)	$\delta\ ^{11}B$ (‰)	$\delta\ ^{13}C[DIC]$ (‰)	$^{14}C[DIC] \pm$ counting error (% modern)	$\delta\ ^{15}N[N_2]$ (‰)	$\delta\ ^{15}N[NO_3]$ (‰)	$\delta\ ^{18}O[NO_3]$ (‰)	$\delta\ ^{34}S[SO_4]$ (‰)	$^{87}Sr/^{86}Sr$
Central High Plains aquifer												
CAL-122	7/10/00	1.5	−61.9	−8.33	–	–	–	–	6.8	–	−45.0, −45.0	–
CNG	7/25/00	<0.3	−56.6	−7.76	–	−4.6	65.09 ± 0.60	–	4.4	–	1.8	–
Rolla-193	8/30/99	0.3	−53.6	−7.84	21.2	−5.0	73.05 ± 0.59	0.52	4.14, 4.04	–	0.1	0.70867
Rolla-366	8/30/99	<0.3	−60.8	−8.46	22.2	−5.4, −5.6	21.12 ± 0.29, 21.82 ± 0.32	0.59, 0.70	6.27, 6.31	–	8.6	0.70839
Hugoton-140	8/29/99	12.3	−49.0	−7.16	22.0	–	–	–	6.70	–	1.6	0.70867
Hugoton-313	8/29/99	<0.3	−56.9	−8.03	14.0	−7.2	14.51 ± 0.21	–	7.23	–	5.1	0.70862
Hugoton-495	8/28/99	<0.3	−57.3	−8.10	13.7	−6.6,−7.1	19.03 ± 0.28, 17.63 ± 0.22	0.54	7.60, 7.45	–	3.9, 3.8	0.70862
Hugoton-617	8/28/99	<0.3	−57.2	−7.95	17.5	−6.0, −6.5	20.26 ± 0.26, 17.50 ± 0.30	0.53	6.98	–	5.1	0.70865
Liberal-160	8/27/99	< 0.3	−48.6	−7.04	8.0	−5.8	38.76 ± 0.36	0.56, 0.60	7.90, 7.61	1.65	1.9	0.70872
Liberal-319	8/27/99	< 0.3	−61.9	−8.91	8.0	−6.8	15.08 ± 0.21	0.24, 0.30	9.41, 9.15	2.11	3.2	0.70859
	10/17/00	–	–	–	–	–	–	0.21, 0.26	–	–	–	–
Liberal-436	8/26/99	< 0.3	−62.4	−8.93	5.2	−6.9	11.44 ± 0.26	0.30	9.99, 9.48, 9.27	2.12	3.0	0.70859
	10/17/00	–	–	–	–	–	–	0.32, 0.35	–	–	–	–
Liberal-570	8/26/99	<0.3	−64.9	−9.32	6.5	−6.2	9.80 ± 0.18	–	11.31, 11.79	4.38	5.5	0.70854
	10/17/00	–	–	–	–	–	–	0.30, 0.24, 0.37, 0.37	–	–	–	–
Cimarron-65	9/1/99	4.4	−49.1	−7.36	15.0	−6.3	67.53 ± 0.62	0.46, 0.38	6.04	0.67	2.8	0.70882
Cimarron-210	8/31/99	<0.3	−57.1	−8.11	13.2	−6.0	40.46 ± 0.49	0.46, 0.57	8.27	1.11	5.0	0.70875
Cimarron-336	9/1/99	<0.3	−63.4, −63.7	−8.97, −8.97	8.7, 9.2	−7.6, −7.8	10.36 ± 0.21, 12.20 ± 0.27	1.03, 1.05, 0.91	9.75, 9.55	2.00	8.3, 8.1	0.70862, 0.70860
Upper Permian-Pennsylvanian aquitard												
Cimarron-436	8/31/99	<0.3	−70.7	−9.89	9.5	−8.0	10.75 ± 0.19	1.69, 1.64	11.13,10.32	2.68	10.7	0.70852
	10/18/00	0.3	−70.6	−9.93	–	−8.0	5.10 ± 0.11	–	–	–	10.9	–

Well name	Depth (m)	Mineralogy	$\delta\ ^{13}C$ (‰)	$\delta\ ^{18}O$ (‰)	$\delta\ ^{34}S$ (‰)	$^{87}Sr/^{86}Sr$
Carbonate minerals						
Rolla	64–67	Calcite	−5.86	–	–	–
	107–110	Calcite	−5.75	–	–	–

Watson	329–332	Dolomite	6.14	36.82	–	–
	369–372	Calcite	−18.15	19.73	–	–
	369–372	Dolomite	−6.29	37.76	–	0.70720
Hugoton	116–119	Calcite	−5.26	–	–	–
	149–152	Calcite	−6.63	–	–	–
	186–189	Calcite	−6.03	–	–	–
Liberal	98–101	Calcite	−5.63	–	–	–
Cimarron	61–64	Calcite	−3.86	–	–	–
	73–76	Calcite	−6.8	–	–	–
	110	Calcite	−6.33, −6.28	23.59, 23.59	–	–
	111	Calcite	−4.27, −4.28	21.45, 21.45	–	–
	115	Calcite	−4.77	24.67	–	–
	115	Dolomite	0.65	28.06	–	–
	129	Dolomite	−0.16	29.97	–	–
Kneeland	354–360	Dolomite	–	–	–	0.70831
Sulfate minerals						
Watson	268–271	Gypsum> anhydrite	–	–	10.7	–
	305–311	Anhydrite≫ gypsum	–	–	12.6, 12.4	–
	329–332	Anhydrite> gypsum	–	–	–	0.70788
Cimarron	114	[a]	–	–	10.2	–
	128	[a]	–	–	9.4	–
	129	[a]	–	–	8.7	–
Kneeland	213–219	Ggypsum≫ anhydrite	–	–	12.9	–
	219–226	Gypsum> anhydrite	–	–	12.8	0.70744
	341–347	Anhydrite> gypsum	–	–	–	0.70821
	396–402	Anhydrite	–	–	–	0.70760

Multiple entries indicate replicate samples. Mineralogy determined by X-ray diffraction analysis.
[a] Hot-water extraction of sediment, sulfate-mineral content too small for X-ray diffraction analysis.

Table 5
Carbonate and organic carbon contents and bulk mineralogy of sediment from the central High Plains aquifer and Upper Permian-Pennsylvanian aquitard

Well name	Depth (m)	General lithology	Carbonate carbon content (wt%)	Organic carbon content (wt%)	Bulk mineralogy
CAL-122	52	Silty clay	1.31	0.43	–
Rolla	110	Medium to coarse sand	–	–	Quartz, potassium feldspar, albite, calcite, muscovite, montmorillonite
Hugoton	61	Medium to coarse sand	3.22	<0.05	–
	73	Sandy clay	1.77	0.06	–
	116	Sandy clay	0.68	0.12	–
	186	Fine to coarse sand	–	–	Quartz, anorthoclase, calcite
Liberal	131	Medium to coarse sand	–	–	Quartz, potassium feldspar, albite, muscovite
	158	Siltstone	<0.02	<0.05	–
Cimarron	24	Sandy clay	1.71	0.60	–
	49	Clayey sand	0.65	0.21	–
	61	Medium to coarse sand	–	–	Quartz, potassium feldspar, albite, calcite, muscovite
	110	Sandy, silty clay	–	–	Quartz, microcline, montmorillonite, muscovite, albite, hematite, chlorite, kaolinite
	129	Siltstone	0.74	0.07	Quartz, dolomite, orthoclase, albite, muscovite, montmorillonite, kaolinite

Mineralogy determined by X-ray diffraction analysis. Minerals listed in order of decreasing abundance.

be the largest O_2 concentration at which some denitrifying bacteria are active (Skerman and MacRae, 1957). Other studies indicate some strains of bacteria actively denitrify at O_2 concentrations up to 220 μM (Frette et al., 1997), well within the range of most of the measured O_2 concentrations.

Nitrate concentrations in the aquifer ranged from about 17 to 408 μM (Table 3) and did not markedly decrease with depth at each site. Values of $\delta\ ^{15}N[NO_3]$ increased with depth at the Rolla, Liberal, and Cimarron sites (Table 4). Those trends in $\delta\ ^{15}N[NO_3]$ values could indicate denitrification (Delwiche and Steyn, 1970; Mariotti et al., 1988) or a change in the N isotopic composition of NO_3 in recharge over time. The fact that the ^{15}N enrichment in NO_3 was accompanied by ^{13}C depletion in DIC (Fig. 4(c)) supports the hypothesis that denitrification occurred in the aquifer. Denitrification commonly is coupled to the oxidation of organic C, a ^{13}C-depleted source of DIC.

Even though there was evidence for O_2 and NO_3 reduction in the aquifer, the reduction rates must have been slow given that both constituents persisted to depths of more than 100 m below the water table. The reduction rates probably were limited by the small quantities of organic C in water and sediments to support microbial metabolism (Tables 3 and 5). The relatively small concentrations of O_2 and NO_3 in water from the Permian-Pennsylvanian aquitard and clays within the aquifer indicate that O_2 reduction and denitrification might have been focused in those deposits or at the contacts between those deposits and coarser grained sediments.

The two deepest wells at the Cimarron site had abnormally large salinities. Cimarron-436 had a total dissolved-solids concentration of 15,400 mg/L (mainly Na-Cl), almost half that of seawater. Chemical and isotopic data indicate water from Cimarron-436 was meteoric in origin and that it acquired its salinity after being recharged. The Br/Cl ratios for water from that well did not resemble those of seawater or oilfield brine from Kansas but were located along a mixing line between freshwater and halite-dissolution brines found in

Table 6
Concentrations of dissolved gases in water from sampled wells in the central High Plains aquifer and Upper Permian-Pennsylvanian aquitard

Well name	Sample date	Elevation of water table in recharge area[a] (m)	$N_{2\text{-TOTAL}}$ (μM)	Ar (μM)	Ne ± 1σ (× 10^{-3} μM)	^{4}He ± 1σ (×10^{-3} μM)	δ ^{3}He ± 1σ (%)	Recharge temperature (°C)	Excess air (cm^3 STP/L)
Central High Plains aquifer									
CAL-122	7/10/00	–	–	–	–	–	–	–	–
CNG	7/25/00	–	–	–	–	–	–	–	–
Rolla-193	8/30/99	990	682	15.95	9.74 ± 0.11[b]	2.04 ± 0.01[b]	−2.9 ± 0.3	–	–
Rolla-366	8/30/99	1035	562, 575, 568	14.05, 14.26, 14.13	8.33 ± 0.10	5.26 ± 0.01	−41.9 ± 0.2	14.3 ± 0.4	0.9 ± 0.1
Hugoton-140	8/29/99	935	–	–	–	–	–	–	–
Hugoton-313	8/29/99	950	612, 599	14.72, 14.52	9.26 ± 0.11	3.93 ± 0.02	−38.2 ± 0.2	14.7 ± 0.5	1.9 ± 0.1
Hugoton-495	8/28/99	995	607, 598, 602	14.74, 14.61, 14.63	9.29 ± 0.12, 9.47 ± 0.11	3.53 ± 0.01, 3.62 ± 0.01	−34.6 ± 0.2, −34.4 ± 0.2	14.5 ± 0.3	2.1 ± 0.2
Hugoton-617	8/28/99	1030	603, 606	14.56, 14.58	9.08 ± 0.11	3.78 ± 0.01	−36.0 ± 0.2	14.1 ± 0.2	1.8 ± 0.1
Liberal-160	8/27/99	915	598, 601	14.42, 14.48	9.37 ± 0.11	1.96 ± 0.01	−4.7 ± 0.3	15.7 ± 0.2	2.1 ± 0.1
Liberal-319	8/27/00	950	637, 635	15.42, 15.41	9.25 ± 0.10	6.66 ± 0.02	−44.5 ± 0.2	11.8 ± 0.2	1.7 ± 0.1
	10/17/00		634	15.36	–	–	–		
Liberal-436	8/26/99	985	634	15.36	–	–	–	11.9 ± 0.1	2.0 ± 0.0
	10/17/00		641	15.44	9.45 ± 0.03	7.49 ± 0.02	−46.9 ± 0.4		
Liberal-570	8/26/99	1030	667	15.59	9.38 ± 0.11	12.4 ± 0. 03	−55.2 ± 0.2	11.1 ± 0.2	1.9 ± 0.2
	10/17/00		673, 676	15.69, 15.72	–	–	–		
Cimarron-65	9/1/99	850	544	13.85	8.04 ± 0.09	3.19 ± 0. 01	−18.2 ± 0.2	15.7 ± 0.2	0.4 ± 0.1
Cimarron-210	8/31/99	975	573, 560	14.15, 13.99	8.35 ± 0.10	8.42 ± 0.03	−52.2 ± 0.2	14.9 ± 0.4	0.9 ± 0.1
Cimarron-336	9/1/99	1035	644, 636, 654	14.98, 14.84, 15.09	8.49 ± 0.04	60.1 ± 0.3	−5.8 ± 0.3	11.6 ± 0.4	0.8 ± 0.1
Upper Permian-Pennsylvanian aquitard									
Cimarron-436	8/31/99	1050	759, 749	16.98, 16.93	10.2 ± 0.05	59.7 ± 0.3	−1.2 ± 0.3	8.0 ± 0.1	2.6 ± 0.1

Well name	$N_{2\text{-ASW}}$ (μM)	$N_{2\text{-EXCESS-AIR}}$ (μM)	$N_{2\text{-EXCESS}}$ (μM)	$N_{2\text{-EXCESS}}$ with bias correction[c] (μM)	δ ^{15}N[$N_{2\text{-EXCESS}}$] (‰)	NO_3, INITIAL (μM)	C/C_0	δ ^{15}N[$NO_{3\text{-INITIAL}}$] (‰)
Central High Plains aquifer								
CAL-122	–	–	–	–	–	–	–	–
CNG	–	–	–	–	–	–	–	–
Rolla-193	–	–	–	–	–	–	–	–
Rolla-366	522 ± 4	30 ± 4	16 ± 6	0	–	162	1.0	6.27, 6.31
Hugoton-140	–	–	–	–	–	–	–	–
Hugoton-313	523 ± 5	68 ± 5	15 ± 8	0	–	183	1.0	7.23
Hugoton-495	522 ± 4	74 ± 7	7 ± 6	0	–	179	1.0	7.60, 7.45

(*continued on next page*)

Table 6 (*continued*)

Well name	$N_{2\text{-ASW}}$ (μM)	$N_{2\text{-EXCESS-AIR}}$ (μM)	$N_{2\text{-EXCESS}}$ (μM)	$N_{2\text{-EXCESS}}$ with bias correction[c] (μM)	δ $^{15}N[N_{2\text{-EXCESS}}]$ (‰)	NO_3, INITIAL (μM)	C/C_0	δ $^{15}N[NO_{3\text{-INITIAL}}]$ (‰)
Hugoton-617	523 ± 2	62 ± 4	19 ± 3	0	–	164	1.0	6.98
Liberal-160	514 ± 2	74 ± 5	11 ± 3	0	–	136	1.0	7.90, 7.61
Liberal-319	555 ± 2	59 ± 4	22 ± 3	12 ± 2	−21 ± 3	249 ± 3	0.90 ± 0.01	6.3 ± 0.4
Liberal-436	551 ± 1	69 ± 1	21 ± 8	11 ± 4	−20 ± 7	241 ± 7	0.91 ± 0.02	6.9 ± 1
Liberal-570	557 ± 2	65 ± 5	49 ± 5	39 ± 4	−5 ± 1	247 ± 7	0.68 ± 0.02	6.3 ± 0.4
Cimarron-65	519 ± 2	14 ± 4	11 ± 3	0	–	148	1.0	6.02
Cimarron-210	519 ± 4	30 ± 4	17 ± 8	0	–	219	1.0	8.25
Cimarron-336	551 ± 4	29 ± 2	65 ± 8	55 ± 7	4 ± 1 (−11 ± 8, 9 ± 3)[d]	274 ± 12 (194 ± 17)[d]	0.60 ± 0.03 (0.85 ± 0.07)[d]	7.4 ± 0.4 (7.0 ± 0.7)[d]
Upper Permian-Pennsylvanian aquitard								
Cimarron-436	590 ± 1	89 ± 2	75 ± 5	65 ± 4	12 ± 1 (−11 ± 8, 13 ± 0.9)[d]	156 ± 7 (32 ± 5)[d]	0.16 ± 0.02 (0.80 ± 0.1)[d]	11.8 ± 0.7 (7.0 ± 0.7)[d]

Multiple entries indicate replicate samples. Methane concentrations were less than 1 μM in all samples. ASW refers to air-saturated water.

[a] Based on MODFLOW/MODPATH simulations.

[b] Gas may be fractionated.

[c] Refer to text.

[d] Value outside parentheses assumes denitrification source of excess N_2 and values inside parentheses assume denitrification and natural gas sources of excess N_2, respectively.

Table 7
Mass transfer of phases calculated using NETPATH, in micromol/kg water (positive for dissolution, negative for precipitation)

Initial well	Final well	Albite	$CaSO_4$	Carbon dioxide	Calcite	Dolomite	Halite	Kaolinite	K feldspar	Lignite	Quartz	Ca–Mg/Na Ex[a]	Cimarron-436[b]
Central High Plains aquifer													
Rolla-193	Rolla-366	199	4248	–	−3475	1434	–	−100	–	73	−383	−35 (1.0)	0.001
CNG	Rolla-366	10	3765	–	−2715	1182	–	−5	–	34	29	469 (1.0)	0.001
Rolla-193	Hugoton-313	550	1024	–	−1731	614	–	−275	–	71	−1059	−782 (1.0)	<0.001
CNG	Hugoton-313	361	540	–	−970	362	–	−180	–	31	−647	−278 (1.0)	<0.001
Rolla-193	Hugoton-495	5	847	20	−1346	507	–	−3	–	79	–	−512 (1.0)	<0.001
CNG	Hugoton-495	22	363	123	−689	255	–	−11	–	40	–	−110 (1.0)	<0.001
Rolla-193	Hugoton-617	9	971	25	−1405	522	–	−5	–	68	–	−510 (1.0)	<0.001
CNG	Hugoton-617	26	487	128	−747	270	–	−13	–	28	<1	−108 (1.0)	<0.001
Rolla-193	Liberal-160	207	–	396	−519	394	–	−104	–	59	–	−741 (0.0)	0.001
Rolla-193	Liberal-319	285	391	–	−1581	707	–	−143	–	168	−537	−519 (1.0)	<0.001
CNG	Liberal-319	34	–	71	−888	454	–	−17	–	128	–	12 (1.0)	< 0.001
Rolla-193	Liberal-436	581	375	–	−1696	658	–	−290	–	172	−1173	−638 (1.0)	<0.001
CNG	Liberal-436	159	–	–	−933	405	–	−79	–	133	−294	−22 (1.0)	<0.001
Rolla-193	Liberal-570	–	662	15	−1449	719	–	<1	–	280	−33	−160 (1.0)	<0.001
CNG	Liberal-570	1	178	110	−783	468	–	<1	–	240	–	249 (1.0)	<0.001
Rolla-193	Cimarron-210	285	482	–	−1005	412	–	−142	–	37	−611	−624 (1.0)	0.005
CNG	Cimarron-210	101	1	–	−251	162	–	−50	–	–	−210	−124 (1.0)	0.005
Rolla-193	Cimarron-336	–	–	392	−1275	364	10,530	−45	90	127	−242	−6161 (0.65)	0.190
CNG	Cimarron-336	–	–	432	−919	242	17,400	−74	148	107	−325	−6528 (0.6)	0.159

Initial well	Final well	$\delta^{13}C$[DIC] (‰) measured	$\delta^{13}C$[DIC] (‰) calculated	$\delta^{34}S[SO_4]$ (‰) measured	$\delta^{34}S[SO_4]$ (‰) calculated	$\delta^{13}C$[Dolomite] (‰)	$\delta^{34}S[CaSO_4]$ (‰)[c]	$\delta^{13}C$[Lignite] (‰)	$\delta^{13}C[CO_2]$ (‰)
Central High Plains aquifer									
Rolla-193	Rolla-366	−5.5	−5.3	8.6	8.6	−3.5	9.1	−25.0	–
CNG	Rolla-366	−5.5	−5.4	8.6	8.6	−4.5	9.9	−25.0	–
Rolla-193	Hugoton-313	−7.2	−6.3	5.1	5.1	−6.3	6.3	−25.0	–
CNG	Hugoton-313	−7.2	−5.4	5.1	5.1	−6.3	9.6	−25.0	–
Rolla-193	Hugoton-495	−6.8	−6.2	3.9	3.9	−6.3	5.0	−25.0	−25.0
CNG	Hugoton-495	−6.8	−5.9	3.9	4.0	−6.3	8.5	−25.0	−25.0
Rolla-193	Hugoton-617	−6.3	−6.0	5.1	5.1	−6.0	6.3	−25.0	−25.0
CNG	Hugoton-617	−6.3	−5.9	5.1	5.1	−6.3	10.0	−25.0	−25.0
Rolla-193	Liberal-160	−5.8	−5.7	1.9	0.7	3.0	–	−25.0	−25.0
Rolla-193	Liberal-319	−6.8	−6.5	3.2	3.1	−6.3	5.0	−25.0	–
CNG	Liberal-319	−6.8	−6.2	3.2	1.8	−6.3	–	−25.0	−25.0
Rolla-193	Liberal-436	−6.9	−6.7	3.0	3.1	−6.3	5.0	−25.0	–

(*continued on next page*)

Table 7 (*continued*)

Initial well	Final well	δ ^{13}C[DIC] measured	δ ^{13}C[DIC] (‰) calculated	δ ^{34}S[SO_4] (‰) measured	δ ^{34}S[SO_4] (‰) calculated	δ ^{13}C[Dolomite] (‰)	δ ^{34}S[$CaSO_4$] (‰)[c]	δ ^{13}C[Lignite] (‰)	δ ^{13}C[CO_2] (‰)
CNG	Liberal-436	−6.9	−6.0	3.0	1.8	−6.3	–	−25.0	–
Rolla-193	Liberal-570	−6.2	−6.1	5.5	5.5	−3.2	7.5	−25.0	−25.0
CNG	Liberal-570	−6.2	−6.2	5.5	4.0	−3.2	12.9	−25.0	−25.0
Rolla-193	Cimarron-210	−6.0	−5.7	5.0	5.1	−5.9	6.7	−25.0	–
CNG	Cimarron-210	−6.0	−4.8	5.0	2.6	−6.3	–	−25.0	–
Rolla-193	Cimarron-336	−7.6	−7.7	8.3	10.1	−1.0	–	−25.0	−25.0
CNG	Cimarron-336	−7.6	−7.7	8.3	8.9	−1.0	–	−25.0	−25.0

Measured values of δ ^{13}C[DIC] and δ ^{34}S[SO_4] versus values calculated on the basis of mass transfers and the indicated isotopic compositions of dolomite, $CaSO_4$, lignite, and CO_2.

[a] Number in parentheses is the fraction of Ca/Na ion exchange (1.0 is pure Ca/Na exchange and 0.0 is pure Mg/Na exchange).

[b] Fraction of Cimarron-436 water in mixture with initial water to account for chloride in final water.

[c] Values may represent mixture of Permian anhydrite/gypsum and calcium-sulfate water from clays within aquifer (see text).

Permian rocks in southwestern Kansas (Fig. 3(c)). Whittemore (1984, 1993) concluded on the basis of Br/Cl ratios and other information that halite dissolution brines in Permian rocks in southwestern Kansas were produced by deeply circulating meteoric water that dissolved Permian evaporite deposits. The δ ^{18}O[H_2O] and δ ^{2}H[H_2O] values for water from Cimarron-436 were located along the global meteoric water line, also supporting the meteoric origin for that water (Fig. 4(d)). The δ ^{11}B value for water from Cimarron-436 (9.5‰) (Table 4) was considerably smaller than the δ ^{11}B of seawater (39‰), providing evidence that the water from that well was not derived from a marine source.

4.2. Recharge temperatures

Ground-water recharge temperatures and concentrations of excess atmospheric gases were estimated from concentrations of dissolved Ne and Ar (Weiss, 1970, 1971; Stute and Schlosser, 1993), assuming total dissolution of excess air incorporated during recharge. The estimated recharge temperatures and concentrations of excess air were used to calculate concentrations of excess N_2 from denitrification and other sources, and to evaluate paleoclimatic variations in recharge conditions. The water-table elevation in the recharge area for each well was estimated by using the cross-sectional model of ground-water flow (see below), with values ranging from 850 to 1050 m (Table 6). For the high-salinity Cimarron wells, provisional recharge temperatures were calculated by making two different assumptions: (1) the samples were recharged with their current salinities, and (2) the samples were recharged as fresh water and acquired salts subsequently by evaporite dissolution.

Calculated recharge temperatures for samples from the High Plains aquifer ranged from 11.1 ± 0.2 to 15.7 ± 0.2 °C; whereas Cimarrion-436 yielded values of 4.4 °C (if recharged with its full complement of salts) to 8.0 °C (if recharged fresh) (Table 6). The higher temperature for Cimarron-436 is considered to be more realistic and gives support to the interpretation that the saline ground waters are meteoric waters that acquired salts in the subsurface. The reported 1-σ uncertainties in recharge temperatures were based only on the reproducibilities of the measured Ne and Ar concentrations.

Recharge temperatures decreased with depth at the Liberal and Cimarron nested-well sites, whereas there was essentially no gradient in recharge temperature with depth at the Hugoton site. As discussed previously, water at the Hugoton site apparently was mixed vertically by irrigation pumping in the vicinity of the well site. The two deepest monitoring wells at the Hugoton site overlapped the screened interval of the irrigation well. On the basis of these recharge temperatures, small amounts of excess air were present in all of the samples from the aquifer (Table 6).

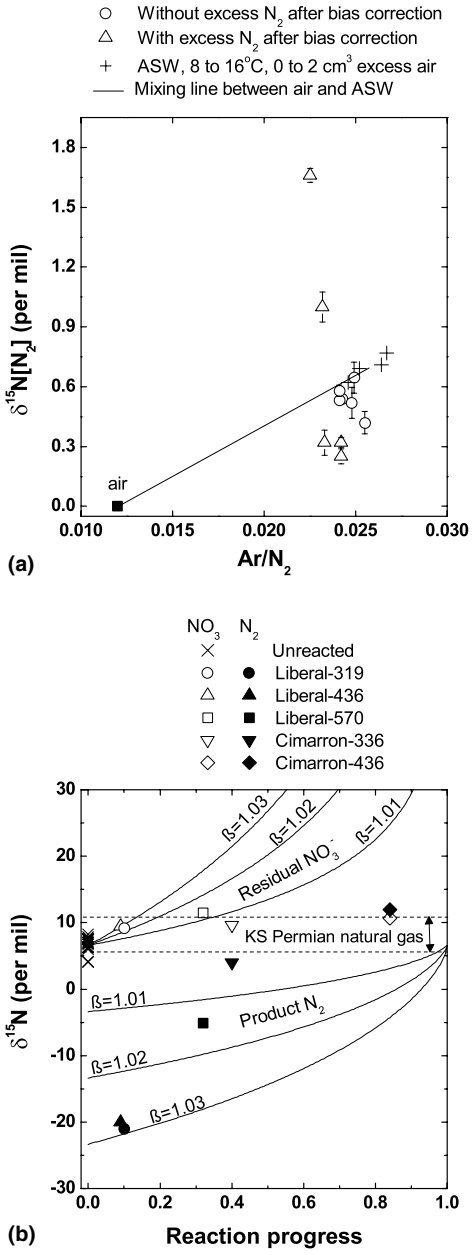

Fig. 5. (a) $\delta\ ^{15}N[N_2]$ versus Ar/N_2 ratios for water samples with and without excess N_2. ASW refers to air-saturated water. (b) $\delta\ ^{15}N$ versus denitrification reaction progress. β refers to the kinetic isotope fractionation factor. The range in $\delta\ ^{15}N[N_2]$ values for Kansas Permian natural gas from Ballentine and Sherwood-Lollar (2002) and D. Newell (Kansas Geological Survey, pers. commun., 2002).

4.3. Evidence for denitrification

The O isotopic composition of NO_3 from the Liberal and Cimarron profiles provides additional evidence for an increase in the progress of denitrification with depth. Variations in $\delta\ ^{15}N$ and $\delta\ ^{18}O$ of NO_3 are correlated and can be fit to a line with a slope of 1:1.7 ($r^2 = 0.82$), which is consistent with isotope fractionation effects of denitrification observed in the laboratory and in aquifers elsewhere (Amberger and Schmidt, 1987; Böttcher et al., 1990; Aravena and Robertson, 1998).

The possibility that denitrification occurred in the aquifer also was evaluated using concentrations of NO_3 and N_2, calculated recharge temperatures and excess air concentrations, and $\delta\ ^{15}N[NO_3]$ and $\delta\ ^{15}N[N_2]$ values. Recharge temperatures were used to calculate the amount of dissolved N_2 from air–water equilibrium, and the excess air concentrations were used to calculate the amount of N_2 from excess air (Table 6). Subtraction of these concentrations from the measured N_2 concentrations provided estimates of the amounts of excess N_2 from non-atmospheric sources. Concentrations of excess N_2 ranged from 7 ± 6 to 75 ± 5 μM (Table 6). The reported 1-σ variability in concentrations of excess N_2 was based on the variability in calculated recharge temperatures and the variability in measured concentrations of total dissolved N_2.

All of the samples had small amounts of excess N_2 on the basis of these calculations (Table 6), even though O_2 concentrations in some of the samples exceeded 200 μM (Table 3), large enough to inhibit denitrification in most aqueous environments. The average concentration of excess N_2 in samples with O_2 >200 μM was approximately 10 μM. The small apparent concentrations of excess N_2 in the oxic samples could represent minor denitrification (e.g., in suboxic subenvironments) or they could indicate there were small biases in the gas ratios caused by either recharge processes (e.g., fractionation of excess air) or analytical inconsistencies (Ar and Ne samples were collected and analyzed using different procedures). To account for a potential systematic bias (assuming oxic samples were not denitrified), an alternative set of minimum excess N_2 concentrations was calculated for all samples by subtracting 10 μM from the measured concentrations (Table 6). Although these alternative calculations do not resolve the presence or absence of excess N_2 in the oxic samples, they are considered to bracket the concentrations of excess N_2 in the sample set as a whole. More rigorous adjustments might be possible with additional noble-gas analyses (e.g., Aeschbach-Hertig et al., 2000), but the excess N_2 concentrations in the oxic samples still would be close to the limit of detection.

At least 5 samples had substantial calculated concentrations of excess N_2 after adjustment to remove 10 μM N_2 from the analyses (Table 6). Those 5 samples had the smallest O_2 concentrations (Table 3), which would be expected in ground water undergoing denitrification. The $\delta\ ^{15}N[N_2]$ and Ar/N_2 values for those 5 samples generally deviated farther from a mixing line between air-saturated water and air than the samples containing

no excess N_2 (Fig. 5(a)), further indicating that those 5 samples contained larger fractions of non-atmospheric excess N_2 than the other samples.

Mass- and isotope-balance calculations were used to determine concentrations of $NO_{3\text{-INITIAL}}$ (C_0), the fraction of unreacted NO_3 (C/C_0), and values of $\delta\ ^{15}N[NO_{3\text{-INITIAL}}]$ and $\delta\ ^{15}N[N_{2\text{-EXCESS}}]$ for the 5 samples containing excess N_2 (assuming the oxic waters had none). Excluding the saline waters from Cimarron-336 and -436, values of $NO_{3\text{-INITIAL}}$, C/C_0, $\delta\ ^{15}N[NO_{3\text{-INITIAL}}]$, and $\delta\ ^{15}N[N_{2\text{-EXCESS}}]$ ranged from 241 ± 7 to 249 ± 3 μM, 0.68 ± 0.02 to 0.91 ± 0.02, 6.3 ± 0.4 to 6.9 ± 1‰, and -21 ± 3 to -5 ± 1‰, respectively (Table 6). The $\delta\ ^{15}N[NO_{3\text{-INITIAL}}]$ values for 3 partially denitrified samples and all samples with $C/C_0 = 1.0$ indicate the N isotope composition of NO_3 in recharge ranged from about 6.0 to 8.2‰ (Table 6). This range in N isotope values is similar to the range in isotope values (6–7‰) for NO_3 extracted from unsaturated-zone cores from near the CNG and CAL-122 sites.

The ^{15}N-enriched residual NO_3 and ^{15}N-depleted excess N_2 in Liberal-319, -436, and -570 (Fig. 5(b)) are consistent with the cumulative effects of kinetic isotope fractionation during denitrification at small to intermediate values of reaction progress, when substantial fractions of the original NO_3 remain (Delwiche and Steyn, 1970; Vogel et al., 1981; Hübner, 1986). $\delta\ ^{15}N$ values for residual NO_3 and excess N_2 for these samples, plotted as a function of reaction progress, are consistent with kinetic isotope fractionation factors, β ($\beta = 1/\alpha$), from about 1.01 to 1.03 (Fig. 5(b)), similar to those in some other denitrifying environments (Delwiche and Steyn, 1970; Hübner, 1986).

In contrast, the $\delta\ ^{15}N[N_{2\text{-EXCESS}}]$ value for Cimarron-436 (12 ± 1‰, Table 6 and Fig. 5(b)) was similar to the measured $\delta\ ^{15}N[NO_3]$ value (10.7 ± 0.5‰) in the same sample (Table 4 and Fig. 5(b)), which is not consistent with water containing NO_3 from a single source that was partially denitrified in a homogeneous closed system. One possible interpretation of these data is that the sample was a mixture of unreacted NO_3 and completely denitrified NO_3 from the same source. This could result from sampling waters from both sides of a sharp denitrification front or from heterogeneous distribution of denitrification sites within the sediments, but these explanations would not be consistent with the data from the other wells. This also would mean that the initial NO_3 in Cimarron-436 was substantially more enriched in ^{15}N than NO_3 in the other samples.

An alternative explanation is that Cimarron-436 contained excess N_2 from two non-atmospheric sources. If it is assumed that one source was denitrification of NO_3 having $\delta\ ^{15}N[NO_{3\text{-INITIAL}}]$ and β values similar to the other samples (approximately 7.0 ± 0.7‰ and 1.02 ± 0.01), values of $\delta\ ^{15}N[N_{2\text{-EXCESS}}]$ and C/C_0 from that source would be -11 ± 8‰ and 0.80 on the basis of Rayleigh fractionation and mass-balance calculations (Table 6). On the basis of these assumptions, the isotopic composition of the second component of non-atmospheric excess N_2 would be 13 ± 0.9‰. For Cimarron-336, the isotopic composition of the second component of excess N_2 would be 9 ± 3‰ (Table 6).

The study area is located within the Hugoton Embayment, which contains one of the largest natural gas reservoirs in the United States. The principal gas-producing zone is in Permian carbonate rocks. Jenden et al. (1988a) report analyses of gas samples from the Permian of Kansas that contained an average of 20.1% N_2 by volume. This is an unusually large N_2 content in comparison to the median N_2 concentration of 3% in over 12,000 natural gas samples from the United States (Jenden et al., 1988b). Kansas Permian gases had measured $\delta\ ^{15}N[N_2]$ values ranging from about 5 to 11‰ (Ballentine and Sherwood-Lollar, 2002; D. Newell, Kansas Geological Survey, personal communication, 2002). These isotope values are similar to the values calculated for the hypothetical second source of excess N_2 in Cimarron-336 and -436 (Table 6). Ballentine and Sherwood-Lollar (2002) report that $\delta\ ^{15}N[N_2]$ values of the Permian gases were inversely correlated with $^4He/N_2$ ratios, with the most ^{15}N-enriched gas samples having $^4He/N_2$ ratios of 0.020. The $^4He/N_2$ ratios of non-atmospheric, non-denitrified gases in Cimarron-336 and -436 (0.0012 and 0.00081) were smaller than the minimum ratios reported by Ballentine and Sherwood-Lollar (2002) and are consistent with the slightly more positive $\delta\ ^{15}N[N_2]$ values reported here. Thus, it is proposed that the deep Cimarron samples may have contained N_2 and ^4He components derived from natural gas in underlying Permian sediments, in addition to atmospheric and denitrification-derived N_2.

4.4. Mass-balance models

The computer program NETPATH (Plummer et al., 1994) was used to develop mass-balance models of the changes in chemical composition of water between recharge and downgradient wells. The number of plausible models was constrained using mineralogic data, mineral saturation indices (SI), and isotope data for dissolved species and solid phases containing C and S. Mass-balance results were used to adjust ^{14}C[DIC] measurements for mass transfers involving C prior to radiocarbon dating.

4.4.1. Mineral phases and mass-balance models

The steps taken to delineate flow paths between recharge and downgradient wells were discussed previously. Even with these steps, it is difficult to establish whether initial and final wells selected for mass-balance modeling were actually aligned along the same flow line. Thus, the chemical and isotope data from Rolla-193 and

CNG were selected to represent the range in compositions of recharge water because (1) their major-ion compositions generally spanned the range of compositions measured in the larger survey of water-table wells, (2) they were the only water-table wells whose ^{3}H values indicated prebomb recharge so their ^{14}C[DIC] compositions were likely not contaminated with postbomb ^{14}C, and (3) flow modeling indicated that water from all of the downgradient wells was recharged upgradient from the other candidate water-table wells. Geochemical mass-balance models assume chemical steady state. In addition, by using 1999 water analyses to represent recharge, we are assuming paleorecharge had the same composition as modern recharge in undisturbed (non-irrigated) locations.

The following phases were included in the mass-balance models: albite, $CaSO_4$ (anhydrite or gypsum), calcite, CO_2, dolomite, kaolinite, N_2, potassium feldspar, SiO_2, Ca–Mg/Na exchange, and lignite. Increases in Cl concentrations along flow paths in the aquifer were attributed to mixing with water from the aquitard. The recharge wells and Cimarron-436 were selected as the end members in those mixtures. The constraints used in the models were concentrations of Na, K, Ca, Mg, Al, Cl, C, N, Si, and redox state of the water.

Several mass-balance models were identified for each pair of initial and final wells; however, constraints imposed by the mineral SI and isotope data eliminated many of them. The mass-balance results listed in Table 7 satisfied most of the constraints imposed by the data. Two models, based on Rolla-193 and CNG as the recharge, are presented for each downgradient well. Most of the models required the dissolution of albite, $CaSO_4$, and dolomite; the precipitation of calcite, kaolinite, and quartz; cation exchange; and mixing with small amounts of water from the Permian aquitard (Cimarron-436) to account for changes in water chemistry between the initial and final wells. The minerals required to dissolve and precipitate to achieve mass balance were consistent with the calculated mineral SI. For Cimarron-336, SO_4 was used to calculate the amount of mixing rather than Cl because models that used Cl to calculate mixing required gypsum to precipitate, which was not supported by the thermodynamic analyses.

Comparisons between the mass-balance models in Table 7 and the models of Fryar et al. (2001) for the southern High Plains indicate a relatively more complicated set of reactions with larger mass transfers was required to account for chemical changes along flow paths in the central High Plains aquifer. Fryar et al. (2001) reported that chemical reactions in the southern High Plains aquifer were negligible or that only CO_2 dissolution, cation exchange, and calcite dissolution were required to account for chemical changes along flow paths. The apparent difference in mass-balance models between the southern and central High Plains aquifers could result from the fact that Fryar et al. (2001) mainly focused on recharge processes, whereas the current study focused on the saturated zone after recharge. In addition, the wells used in the southern High Plains study were shallower and had longer screened intervals than the wells used in this study. Shallower wells probably intercept water with shorter residence times, and the longer screened intervals could result in vertical mixing that can mask vertical gradients in chemistry (Fryar et al., 2001).

Small additions of CO_2 were required to achieve mass balance in a few of the models (Table 7), even though the system below the water table is considered closed to exchange of CO_2 gas with the soil atmosphere. The median CO_2 addition (117 μmol/kg) was equivalent to 3% of the median DIC concentration in recharge and is probably well within the combined uncertainties in (a) selecting the appropriate recharge water for the downgradient wells, (b) the DIC analyses, and (c) the charge imbalance of the major-ion analyses. Plummer and Sprinkle (2001) presented mass-balance models that required small additions of CO_2 along flow paths in confined parts of the Upper Floridan aquifer, which was considered closed to soil-zone CO_2. They proposed that small CO_2 additions in the modeled waters could indicate evolution from recharge waters that had slightly larger DIC concentrations than used in the models. Given the uncertainties in the chemical and isotope data, the CO_2 additions required by some models in this study are not considered large enough to invalidate the mass-balance models.

It is unlikely that the relatively larger CO_2 additions required in models of Cimarron-336 (Table 7) indicate upward leakage of CO_2 from underlying Permian natural-gas deposits, as occurred with N_2, because the CO_2 content of those gas deposits generally is 1–3 orders of magnitude smaller than the N_2 content (Jenden et al., 1988a). It is more likely that the larger CO_2 additions reflect uncertainty in the chemical composition of aquitard water that was mixed with Cimarron-336 water. Models for Cimarron-336 required mixing with l6–19% aquitard water, whereas the other wells required mixing with <1% aquitard water (Table 7). The larger percentage of aquitard water in Cimarron-336 reflects its location in the Cimarron River valley, which is a regional ground-water discharge area. This evaluation is consistent with the upward hydraulic gradient between Cimarron-436 and -336 (McMahon, 2001).

The large mass transfer of halite required in models for Cimarron-336 also could reflect uncertainty in the chemical composition of aquitard water used in the mixing calculations. Removing Cl from the mass-balance calculations eliminated the halite and CO_2 mass transfers from both models for Cimarron-336 and resulted in only a 2–14% increase in calculated radiocarbon ages.

Lignite oxidation required to achieve mass balance was coupled to O_2 reduction and denitrification. It was not possible to know the O_2 concentration in the downgradient well water at the time it was recharged; therefore, the amount of O_2 reduction was calculated as the difference in O_2 concentrations between the recharge and downgradient wells (Table 3). The amount of denitrification was assumed to equal the amount of excess N_2–N present in the downgradient wells, as previously discussed (Table 6). Thus, for calculating mass balances between recharge and downgradient well pairs, the NO_3 concentration in the recharge well was set equal to $NO_{3\text{-INITIAL}}$ in the downgradient well (Table 6). The only other redox reaction in the aquifer that had a noticeable effect on water chemistry was trace amounts of Mn reduction (Table 3), which was not included in the mass-balance calculations.

4.4.2. Isotope constraints

Plausible mass-balance models also were evaluated with respect to the constraints imposed by isotope data for dissolved species and solid phases containing C and S. The species for which isotope data were available included DIC, SO_4, $CaSO_4$, calcite, and dolomite (Table 4). The δ ^{13}C composition of lignite was assumed to be −25‰, a reasonable approximation for terrestrial organic matter (Deines, 1980). The model values of δ ^{34}S[$CaSO_4$] required to achieve a match between measured and calculated δ ^{34}S[SO_4] values ranged from 5 to 12.9‰ (Table 7). The models involving CNG as the initial water and the Liberal wells as the final waters required little or no $CaSO_4$dissolution (Table 7); therefore, an acceptable match between measured and calculated δ ^{34}S[SO_4] values was not achieved in those cases. However, acceptable matches were achieved for models involving Rolla-193 as the initial water. As previously discussed, there are two likely sources of SO_4 in the aquifer: (a) Permian anhydrite/gypsum (10.7–12.9‰) and (b) Ca–SO_4 waters in clays in the aquifer (−45‰) (Fig. 4(a)); therefore the model values of δ ^{34}S[$CaSO_4$] less than about 10.5‰ are consistent with a mixture of those two SO_4 sources. On the basis of the model values of δ ^{34}S[$CaSO_4$], $CaSO_4$mass transfers, and the average δ ^{34}S compositions of Permian anhydrite/gypsum (12.3‰) and SO_4 from clays (−45‰), the Permian anhydrite/gypsum accounted for 87–100% of the SO_4 inputs.

Model values of δ ^{13}C[dolomite] were allowed to vary within the range of measured values (−6.29–6.14‰) (Table 4) to obtain a match between measured and calculated δ ^{13}C[DIC] values. The difference between measured and calculated δ ^{13}C[DIC] values was 0.2‰ or less in 8 models, greater than 0.2 and less than 1.0‰ in 9 models, and 1–2‰ in 2 models (Table 7). The differences larger than 0.2‰ could result from uncertainty in the δ ^{13}C[DIC] value for recharge. The two wells used to represent recharge (CNG and Rolla-193) had δ ^{13}C[DIC] values of −4.6 and −5.0‰ (Table 4), whereas another water-table well (Cimarron-65) had a δ ^{13}C[DIC] value of −6.3‰. If δ ^{13}C[DIC] equal to −6.3‰ was used to represent recharge in those cases where the difference between measured and calculated δ ^{13}C[DIC] values was greater than 0.2‰, the difference between measured and calculated δ ^{13}C[DIC] values would have been less than 0.2‰ in all cases. The magnitude of the δ ^{13}C[DIC] differences could also have been reduced if δ ^{13}C[dolomite] values less than −6.3‰ were allowed. The smallest δ ^{13}C[dolomite] value required to precisely match measured and calculated δ ^{13}C[DIC] values was −14‰. Parkhurst et al. (1992) reported δ ^{13}C[dolomite] values as low as −15.8‰ in sediments of Permian age in central Oklahoma.

4.4.3. Mineral constraints

Anhydrite, gypsum, and dolomite were detected in aquitard sediments by using XRD analysis, but they were not detected in the 4 samples of aquifer sediment subjected to XRD analysis (Tables 4 and 5). The detection limit for an individual mineral type in bulk sediment using XRD analysis is about 1 wt% or more (Breit et al., 1990). Thus, it is possible that the abundances of these minerals in the aquifer were smaller than the XRD detection limit, or that the limited number of samples analyzed was not representative of the anhydrite and dolomite content of the aquifer sediments as a whole. Assuming a sediment porosity of 0.33 and an average grain density of 2.65 g cm^{-3}, the median anhydrite and dolomite mass transfers needed to achieve mass balance (514 and 454 μmol kg^{-1} water) (Table 7) would require anhydrite and dolomite contents in the sediment of less than 0.005 wt%. This calculation indicates that only small amounts of those minerals were needed to satisfy the mass-balance requirements. About 3 wt% of anhydrite and dolomite would have dissolved during the history of the aquifer, assuming the sediments are 20 Ma old and a ground-water turnover time of 10 ka. Reworked sediments of Permian age containing anhydrite and dolomite have been reported in sands and gravels in the aquifer (Smith, 1940). An analog to this occurs in the southern High Plains aquifer, where the authors have observed oyster shells derived from underlying sediments of Cretaceous age in drill cuttings from throughout the thickness of the aquifer. Eolian deposition, which has occurred across the High Plains, also could have delivered trace amounts of anhydrite and dolomite to the area during deposition of the aquifer sediments. Potential source areas include outcrops of sediments of Permian age to the east, south, and southwest of the study area. The White Sands National Monument in southern New Mexico, where the dune sands are essentially pure gypsum, is an example of the transport and deposition of a highly reactive mineral phase by eolian processes.

Mass-balance models that did not contain dolomite as a mineral phase but did satisfy constraints imposed by the isotope data were produced for some flow paths. Those models did not require dissolution of any carbonate mineral, but they did require larger inputs of CO_2 than were required by the models in Table 7. Redox processes that were identified on the basis of water chemistry and were capable of producing CO_2 (O_2 reduction and denitrification) were already accounted for in the mass-balance models by lignite oxidation, so the source of the additional CO_2 is problematic. The amount of Mn reduction indicated by the trace concentrations of dissolved Mn was insufficient to produce the additional CO_2. One consequence of having no carbonate dissolution in the models that excluded dolomite was that the adjusted radiocarbon ages were about 2000 ka older than the ages determined using the models with dolomite. A similar shift toward older radiocarbon ages was obtained for all of the downgradient wells when carbonate dissolution was not included in the mass-balance models; therefore, the relative differences in ages between the wells did not change substantially for models that did or did not contain dolomite.

The model predictions of calcite precipitation along flow paths were consistent with the presence of calcite cements in cuttings and core of the aquifer and aquitard sediments. The $\delta\ ^{13}C$ values of precipitating calcite, as calculated in NETPATH using the Mook set of fractionation factors (Plummer et al., 1994), ranged from −6.5 to −4.1‰. This range in $\delta\ ^{13}C$ values is in good agreement with the measured $\delta\ ^{13}C$[calcite] values of −6.8 to −3.9‰ (Table 4). One sample of calcite cement from the aquitard had a $\delta\ ^{13}C$[calcite] value of −18.1‰, indicating a significantly larger component of C derived from organic sources than was observed in the aquifer.

The processes of dedolomitization, cation exchange, O_2 reduction, denitrification, silicate mineral weathering, and mixing with small percentages of Permian-Pennsylvanian aquitard water satisfied most of the constraints imposed by the mineral SI, mineralogic, and isotope data. However, as the preceding discussion illustrates, those mass-balance reactions should be considered non-unique because small variations in several of the model parameters (mineralogy, isotope composition of water and minerals, chemical composition of recharge) could provide similar matches between measured and calculated values. However, none of the variations in model parameters that satisfied the model constraints produced substantially different results in the radiocarbon ages.

4.5. Radiocarbon ages

Adjusted radiocarbon ages of ground water were calculated using the computer program NETPATH (Plummer et al., 1994) and the radioactive decay equation

$$\Delta t = \frac{5730}{\ln 2} \ln\left(\frac{A_{nd}}{A}\right), \quad (1)$$

where Δt (in years) is the time since ground water was isolated from the atmosphere, 5730 is the half-life of ^{14}C (in years), A_{nd} (in percent modern C, pmc) is the ^{14}C[DIC] value at the final well adjusted for C mass transfers in the absence of radioactive decay, and A (in pmc) is the measured value of ^{14}C[DIC] in the final well. The value of A_{nd} is dependent on the value of A_0 (the ^{14}C[DIC] value in recharge) and the C mass transfers calculated in the mass-balance models (Table 7).

In this study, A_0 was measured directly in the water-table wells Rolla-193 and CNG. Direct measurements of A_0 must avoid water containing a component of ^{14}C derived from atmospheric nuclear weapons testing (as indicated by the presence of elevated ^{3}H concentrations in water). Both water-table wells were screened within 3 m of the water table (Table 1) and contained prebomb concentrations of ^{3}H (Table 4), assuming that precipitation in the High Plains contained about 8 TU of ^{3}H prior to the onset of weapons testing (Thatcher, 1962). For comparison, values of A_0 equal to 100 pmc and values calculated in NETPATH using a mass-balance method (Plummer et al., 1994) also were used to calculate radiocarbon ages. The radiocarbon ages presented here do not account for the possibility that ^{14}C[DIC] of recharge varied over time due to variations in the Earth's geomagnetic field strength and solar fluctuations (Mazaud et al., 1991; Bard et al., 1993).

Radiocarbon ages calculated using these A_0 values are listed in Table 8. The 1-σ uncertainty in the average adjusted radiocarbon age calculated using the measured A_0 values was about ±100 a, based on the difference in measured A_0 values in the two recharge wells. Another source of uncertainty in the radiocarbon ages was associated with the combined precision of the ^{14}C sample collection and analysis. The uncertainty in the ages was estimated to be about ±800 a, on the basis of the average percent difference in ^{14}C[DIC] values (10%) between 4 pairs of replicate analyses (Table 4). The combined uncertainty in the radiocarbon ages was estimated to be about ±900 a for calculations using measured A_0 values. Additional errors in the radiocarbon ages may be associated with the validity of the mass-balance models (Table 7) used to calculate A_{nd}. Corrections for matrix diffusion (molecular diffusion of ^{14}C[DIC] from aquifers to aquitards) were not made in this study but could lead to younger adjusted ages than those reported in Table 8 (Bethke and Johnson, 2002). The magnitude of the correction depends on the relative thickness of interbedded sand and clay layers (Sanford, 1997). The median thickness of sands screened in this

Table 8
Summary of radiocarbon ages and ground-water velocities

Initial well	Final well	Unadjusted age		Adjusted age (NETPATH)						Flow-path length (m)	Ground-water velocity (m/a)
		^{14}C[DIC] measured in final well (pmc)	Age [a] (^{14}C years B.P.)	A_0 mass balance[b] (pmc)	Calculated A_{nd} (pmc)	Age (^{14}C years B.P.)	A_0 Measured (pmc)	Calculated A_{nd} (pmc)	Age (^{14}C years B.P.)		
Rolla-193	Rolla-366	21.5	12,700	70	28.5	2300	73	30.1	2800	–	–
CNG	Rolla-366	21.5	12,700	60	28.4	2300	65	30.8	3,000		
Rolla-193	Hugoton-313	14.5	16,000	70	47.3	9800	73	49.7	10,200	–	–
CNG	Hugoton-313	14.5	16,000	60	47.8	9900	65	51.6	10,500		
Rolla-193	Hugoton-495	18.3	14,000	70	50.5	8400	73	53.0	8,800	–	–
CNG	Hugoton-495	18.3	14,000	60	49.4	8200	65	53.3	8,800		
Rolla-193	Hugoton-617	18.9	13,800	70	50.6	8200	73	53.2	8,600	–	–
CNG	Hugoton-617	18.9	13,800	60	48.9	7900	65	52.8	8500		
Rolla-193	Liberal-160	38.8	7800	70	50.3	2200	73	53.3	2600	38,400	15
Rolla-193	Liberal-319	15.1	15,600	70	44.9	9000	73	47.0	9400	54,300	6
CNG	Liberal-319	15.1	15,600	60	43.9	8,800	65	47.4	9500		
Rolla-193	Liberal-436	11.4	18,000	70	45.5	11,400	73	47.7	11,800	70,700	6
CNG	Liberal-436	11.4	18,000	60	45.7	11,400	65	49.2	12,100		
Rolla-193	Liberal-570	9.8	19,000	70	43.7	12,400	73	45.9	12,800	88,700	7
CNG	Liberal-570	9.8	19,000	60	42.2	12,100	65	45.6	12,700		
Rolla-193	Cimarron-210	40.5	7500	70	51.9	2100	73	57.0	2800	–	–
CNG	Cimarron-210	40.5	7500	60	51.7	2000	65	59.0	3,100		
Rolla-193	Cimarron-336	11.3	18,000	70	42.6	11,000	73	44.6	11,400	–	–
CNG	Cimarron-336	11.3	18,000	60	39.9	10,400	65	43.0	11,100		

Ground-water velocities were calculated using average adjusted radiocarbon ages (measured A_0) and flow-path lengths determined from ground-water flow simulations.
[a] Unadjusted age calculated assuming $A_0 = A_{nd} = 100$ pmc.
[b] Mass-balance model in NETPATH for defining A_0. The model assumes ^{14}C[carbonates] = 0 pmc, ^{14}C[CO_2] = 100 pmc.

study was 15 m. Examination of resistivity logs from boreholes along the transect indicated the median clay thickness was 1.2 m. Using these thicknesses in the correction equation of Sanford (1997) indicates matrix diffusion could reduce adjusted radiocarbon ages by 20%.

The adjusted radiocarbon ages (A_0 measured) of water from the transect wells ranged from 2600 to 12,800 (^{14}C) a B.P. (Table 8). Water from Hugoton-140 and Cimarron-65 contained postbomb ^{3}H; therefore, radiocarbon dating was not attempted for those wells. Ground-water ages increased with depth below the water table at all of the sites except Hugoton (Fig. 6), where relatively young apparent ages in the two deepest wells are attributed to vertical mixing caused by pumping of a nearby irrigation well. Water from Rolla-366 and Cimarron-210 had ages that were considerably younger than water from Hugoton-313 and Liberal-319, even though all of these wells were screened about 45 m below the water table (Fig. 6). The relatively young age of water from Rolla-336 may be a result of its location near the upgradient end of the flow system where flow paths were relatively short. Cimarron-210 is located in a regional discharge area; however, the young age of water from that well may indicate deeper penetration of local flow systems in the Cimarron River valley compared to the upland areas because of increased topographic relief in the valley. The flow system in the Cimarron valley may be further complicated by the convergence of several regional flow paths in that area of ground-water discharge. The relatively old ages of water from Hugoton-313 and Liberal-319 may be related to their locations on long flow paths less affected by local flow systems. The age of the oldest sampled waters from the aquifer, 11.8–12.8 ka (^{14}C) B.P., is somewhat younger than the last glacial maximum (about 18 ka [^{14}C] B.P). Several confined aquifers have been reported to contain recharge from the last glacial maximum (Stute et al., 1992, 1995; Plummer and Sprinkle, 2001). Apparently, recharge rates in the unconfined central High Plains aquifer during Holocene time were large enough to flush older recharge from the aquifer.

Average Holocene recharge rates were evaluated through calibration of the MODFLOW/MODPATH models using the adjusted radiocarbon ages. This differs from previous approaches for estimating recharge to the High Plains aquifer, which primarily relied on water-budget methods or flow models calibrated using hydraulic-head data. The initial MODFLOW/MODPATH simulation, based on the average recharge rate of 19 mm/a from Gutentag et al. (1984), resulted in acceptable matches with measured hydraulic heads, but the model-computed ground-water ages were much younger than the radiocarbon ages (Fig. 7). After the initial simulation, recharge and hydraulic conductivity were decreased together to keep the model-computed heads approximately equal to the 1980 measured heads. The result was a reduction in the modeled velocity of ground water and an increase in the modeled ground-water ages. Optimization of the match between radiocarbon and MODPATH particle ages was achieved by assigning contrasting recharge rates to areas overlain by dune

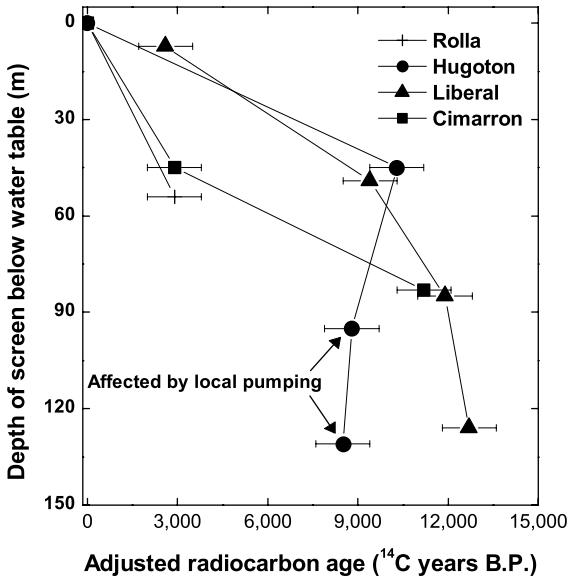

Fig. 6. Vertical distribution of adjusted radiocarbon ages in the aquifer at each transect-well site.

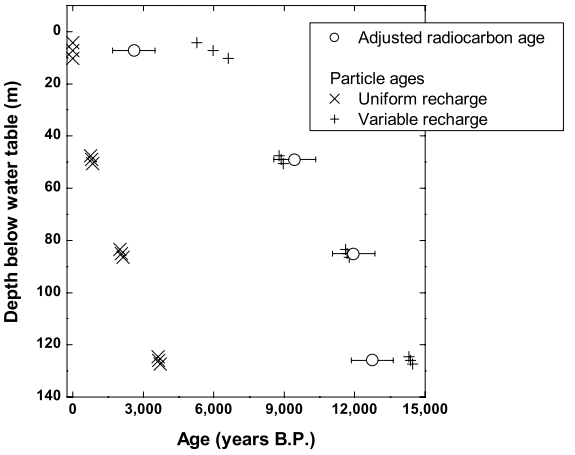

Fig. 7. Adjusted radiocarbon ages and particle ages determined by MODFLOW/MODPATH modeling plotted as a function of depth below the water table at the Liberal well site. Uniform recharge rate used in simulations was 19 mm/a. Variable recharge rates used in simulations were 0.8 mm/a in surficial loess and 8 mm/a in surficial dune sand. The 3 particle ages for each well screen correspond to the top, middle, and bottom of the screen.

sand and to areas overlain by loess (Fig. 2), based on the work of Luckey and Becker (1999). Luckey and Becker (1999) used recharge rates of 18 mm/a in dune areas and 1.7 mm/a in loess areas in a regional ground-water flow model of the aquifer. These rates were adjusted downward in the High Plains transect model in order to optimize the match between radiocarbon and particle ages, preserving the order of magnitude difference in recharge rates between dune and non-dune areas. Recharge ranged from 0.8 to 8 mm/a in the calibrated flow model. These recharge rates were at the lower end of the range of recharge for the High Plains aquifer summarized by Gutentag et al. (1984) but were similar to the long-term average recharge of 1 mm/a estimated by Meyer et al. (1970) using ground-water levels to calculate the change in water in storage and a mass-balance calculation to determine recharge. The average recharge rate for this study, weighted on the basis of dune/loess surface areas, was 3.7 mm/a. This rate compares favorably with an average recharge rate of 5.1 mm/a under rangeland in southwestern Kansas estimated on the basis of a Cl mass-balance in the unsaturated zone (McMahon et al., 2003).

The final calibration was achieved when the ground-water ages determined by particle tracking were in general agreement with the radiocarbon ages, with emphasis on the Liberal site for ages ranging from 2.6 to 12.8 ka (^{14}C) B.P. (Fig. 7). The Liberal site was selected for primary consideration because it was not close to pumping wells that could alter the ground-water flow field (as was the Hugoton site); also, the Liberal site was near the middle of the transect, and it did not appear to be affected by local flow systems or convergence of regional flow paths near discharge areas (as was the Cimarron site). Flow-path lengths for the Liberal sites, calculated in the MODFLOW/MODPATH simulations, ranged from 38.4 to 88.7 km (Fig. 2 and Table 8). Ground-water velocities calculated using the adjusted radiocarbon ages and flow-path lengths ranged from 6 to 15 m/a (Table 8).

Factors that may introduce errors in the matches between radiocarbon and particle ages included a lack of sensitivity in the model to local variations in the ground-water flow system. For example, water from the shallowest well at the Cimarron site contained 4.4 TU of ^{3}H, but the model-calculated age ranged from 1.728 to 5.245 ka B.P. As previously discussed, local flow systems probably affected ground-water ages at that site. Another reason for errors between the radiocarbon and particle ages is the fact that the distribution of hydraulic conductivity and porosity in the High Plains aquifer is complex, whereas the distribution of those parameters in the model is simplified. Dispersion can result in a ^{14}C apparent age that is different from the mean age of a water sample. In addition, it is possible that recharge was not constant over time, as assumed in the model.

4.5.1. Paleorecharge conditions

Recharge temperatures calculated from the measured concentrations of Ar and Ne were separated into two groups on the basis of their radiocarbon ages (Fig. 8(a)). Group 1 waters had an average recharge temperature of 15.2 ± 0.7 °C and radiocarbon ages less than about 3 ka (^{14}C) B.P. Group 2 waters had an average recharge temperature of 11.6 ± 0.4 °C and radiocarbon ages between 9.4 and 12.8 ka (^{14}C) B.P. The Hugoton-313 sample was excluding from these groupings because it may have been affected by local well pumping. The radiocarbon ages indicate group 1 waters were recharged during Late Holocene time and group 2 waters were recharged during Late Pleistocene or Early Holocene time. Recharge temperatures generally are similar to mean annual air temperatures plus 1 to 2 °C (Stute et al., 1995). Thus, the average recharge temperature for the group 1 waters is reasonably consistent with the 100-a mean annual air temperature (13.2 °C) measured at a weather station located 18 km west of the CNG site (High Plains Regional Climate Center, 2002) and centrally located among the simulated recharge areas.

The apparent difference in recharge temperatures between the group 1 and 2 waters was 3.6 ± 0.7 °C. Recharge temperatures are influenced by the elevation of the recharge area as well as climatic variability. Thus, elevation differences between recharge sites could account for some of the observed temperature difference. The maximum difference in elevation of the recharge areas was about 200 m (Table 6). Assuming an air temperature-elevation gradient of −0.6 °C/100 m, elevation differences could account for about 1.2 °C of the observed temperature difference. The temperature-elevation gradient was calculated on the basis of 50 a of temperature data collected at 8 sites in southwestern Kansas and southeastern Colorado (High Plains Regional Climate Center, 2002). Taking into account elevation differences between the recharge areas, the difference in recharge temperatures attributed to the difference in age between group 1 and 2 waters was more likely about 2.4 ± 0.7 °C. This temperature difference between Late Holocene and Late Pleistocene/Early Holocene recharge in the stratified unconfined High Plains aquifer is consistent with the temperature differences estimated for recharge during the same time periods in confined aquifers in southern Texas (about 4 °C) (Stute et al., 1992) and northwestern New Mexico (about 2 °C) (Stute et al., 1995). However, the temperature difference is less than was reported for recharge during the Late Holocene and last glacial maximum in those same confined aquifers (5.2–5.5 °C) (Stute et al., 1992, 1995). The temperature difference between group 1 waters and Cimarron-436 (6.0 ± 0.7 °C after accounting for variable recharge elevations) is similar to the Late Holocene/last glacial maximum temperature differences reported by Stute et al. (1992, 1995), possibly indicating

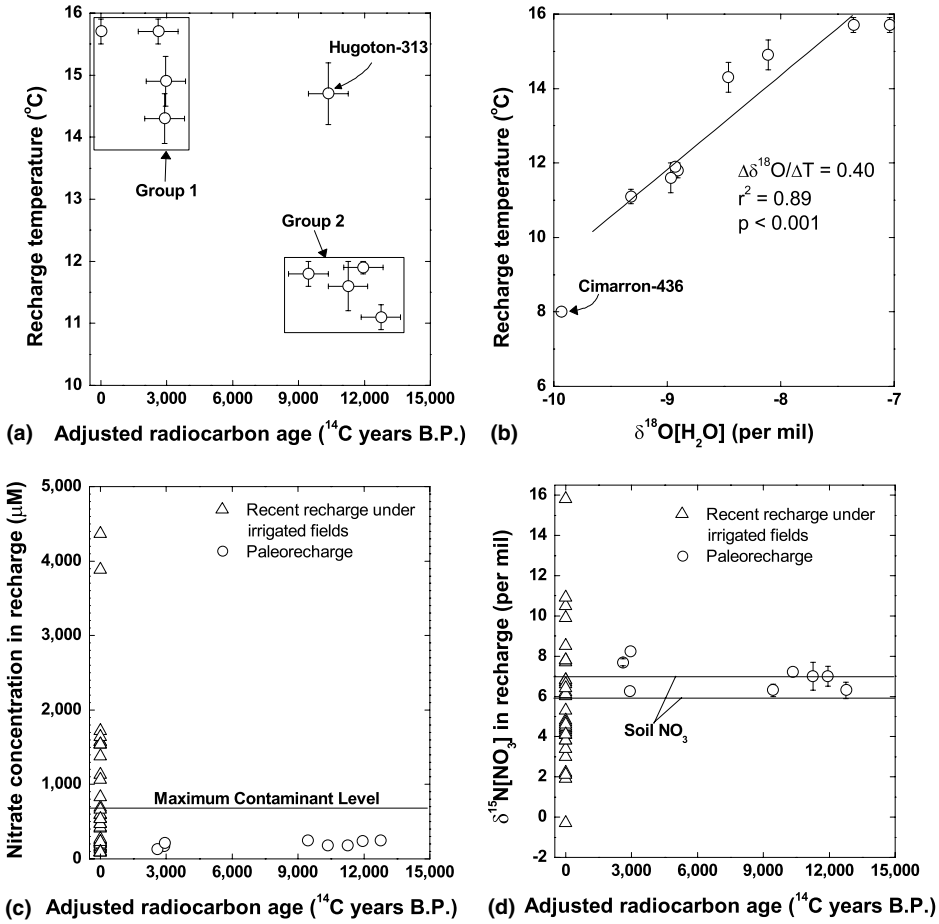

Fig. 8. Recharge temperature versus (a), adjusted radiocarbon age and (b), δ $^{18}O[H_2O]$, (c) NO_3 concentration in recharge versus adjusted radiocarbon age, and (d), δ $^{15}N[NO_3]$ values in recharge versus adjusted radiocarbon age. Data for recent recharge under irrigated fields from Bruce et al. (2003). Maximum Contaminant Level in (c) refers to US Environmental Protection Agency standard for NO_3 in drinking water.

recharge from the last glacial maximum was still present in the aquitard. This interpretation is consistent with the relatively long simulated flow path for Cimarron-436 (Fig. 2); however, interpretation of data from the aquitard is complicated because flowpaths (and mixing) in that unit are not well understood.

The data in Fig. 8(a) indicate a shift from cooler conditions in the Late Pleistocene/Early Holocene to warmer conditions occurred after about 9 ka (^{14}C) B.P., which is consistent with paleoclimatic interpretations based on geomorphic and δ ^{13}C data from southwestern Kansas (Olson et al., 1997; Olson and Porter, 2002). Olson et al. (1997) and Olson and Porter (2002) reported a shift from cooler, wetter climatic conditions to a warmer, drier climate by about 6 ka (calendar) B.P. The occurrence of a climatic shift in southwestern Kansas by the Middle Holocene suggests recharge was not constant throughout Holocene time. The ground-water age distribution at the Liberal site (Fig. 7) corroborates this idea by showing that at least 60% of the saturated thickness at that location contained water recharged more than 9 ka (^{14}C) B.P., presumably during a time when the climate in southwestern Kansas was cooler and wetter than it is now. Additional radiocarbon ages are needed to further evaluate temporal variability in recharge rates during the Holocene in the study area.

Paleorecharge in the High Plains transect was depleted in ^{18}O relative to recent recharge by about 2 (aquifer samples) to 3‰ (Cimarron-436) (Fig. 8(b)). The aquitard water sample was more depleted in ^{18}O than any of the samples from the aquifer, further supporting the possibility that water recharged during the last glacial maximum was still present in the aquitard. These δ ^{18}O data are consistent with the data from Dutton (1995) and Clark et al. (1998) who also reported the presence of ^{18}O-depleted paleorecharge in ground water

from the central High Plains. The aquifer data in Fig. 8(b) yield a δ ^{18}O-temperature relation of 0.4‰ / °C ($r^2 = 0.89$, $p < 0.001$). The relatively strong δ ^{18}O-temperature correlation indicates it might be suitable for estimating paleorecharge temperatures in other water samples from the central High Plains aquifer for which δ ^{18}O data are available.

Nitrate concentrations in paleorecharge had a narrow range (136–249 μM) and small average (193 μM) compared to NO_3 concentrations in recent recharge under irrigated fields in the central High Plains (range = 91–4364 μM, average = 885 μM) (Fig. 8(c)). Recent recharge is defined as water that contained >0.5 TU ^{3}H and/or measurable pesticide concentrations. Similarly, the range in δ ^{15}N[NO_3] values in paleorecharge was narrow (6.3–8.2‰) compared to the range in values for recent recharge under irrigated fields (−0.3–15.8‰) (Fig. 8(d)). Samples of recent recharge containing <60 μM O_2 were excluded from Fig. 8(d) to minimize the influence of denitrification on the plotted distribution of δ ^{15}N[NO_3] values. The range in δ ^{15}N[NO_3] values in paleorecharge was similar to the range in N isotope values for NO_3 in the unsaturated zone in the study area. These data indicate that NO_3, presumably produced naturally in soils, was present in recharge since at least about 12 ka ago. Recently, additional anthropogenic NO_3 with more variable δ ^{15}N values has been recharged in irrigated areas, indicating that other N sources, such as fertilizer and manure, also were important in that land-use setting.

The larger average NO_3 concentration in recharge under irrigated fields compared to paleorecharge is not surprising given the large amounts of water and N applied to irrigated fields relative to natural grasslands in the High Plains, and it indicates irrigated agriculture in the region has increased the flux of NO_3 to the aquifer. Increased input of NO_3 to the aquifer could be problematic from a drinking-water-quality standpoint because of the limited capacity of the aquifer for denitrification. Estimates of denitrification rates in the aquifer were made by using the values of $NO_{3\text{-INITIAL}}$ and C/C_0 (Table 6) and adjusted radiocarbon ages (Table 8). Denitrification was assumed to occur uniformly along flow paths beginning 3 ka (^{14}C) after recharge, which represents the longest residence time of water samples that were not partially denitrified and not affected by local well pumping. Denitrification rates averaged $5 \pm 2 \times 10^{-3}$ μmol N L^{-1} $a^{-1}$for the 4 aquifer samples having C/C_0<1. These rates are lower than estimated denitrification rates ($3 \pm 1 \times 10^{-2}$ μmol N L^{-1} a^{-1}) in an aquifer containing Pleistocene-aged recharge in the Kalahari region of Africa (Vogel et al., 1981). For comparison, denitrification rates were >1000 μmol N L^{-1} a^{-1}in several shallow aquifers containing recent recharge (Korom, 1992). The denitrification rate estimated for the central High Plains aquifer indicates this process would require >10 ka to reduce the average NO_3 concentration in recent recharge under irrigated fields to the natural (Holocene) background concentration.

5. Conclusions

Mass-balance models indicate the primary reactions controlling water chemistry in the central High Plains aquifer were dedolomitization (dolomite dissolution and calcite precipitation driven by anhydrite dissolution), cation exchange, silicate mineral weathering, and O_2 reduction and denitrification. The use of C, S, and Sr isotopes to identify some of these reactions was crucial because of the apparent scarcity of anhydrite/gypsum and dolomite in the clastic aquifer. Dissolved-gas data and isotopes indicate as many as 4 components of N_2 in deep ground water: air-equilibration, excess air, denitrification, and N_2-rich natural gas.

Recharge temperatures calculated using the measured concentrations of Ar and Ne were separated into two groups on the basis of their radiocarbon ages. Group 1 waters had an average recharge temperature of 15.2 ± 0.7 °C and radiocarbon ages less than 3 ka (^{14}C) B.P. and group 2 waters had an average recharge temperature of 11.6 ± 0.4 °C and radiocarbon ages between 9.4 and 12.8 ka (^{14}C) B.P. These data indicate a shift from cooler to warmer conditions occurred after about 9 ka (^{14}C) B.P., which is consistent with previously published data from the area. A cross-sectional model of ground-water flow was calibrated with respect to hydraulic heads and radiocarbon ages by applying a bimodal spatial distribution of recharge rates: 0.8 mm/a in areas overlain by loess and 8 mm/a in areas overlain by dune sand. Calibration of the flow model using radiocarbon ages provided a constraint on the recharge rates that was not possible with other available data and resulted in a 50% decrease in modeled recharge rates compared to previous model estimates. Temporal variations in recharge during Holocene time could not be addressed with the steady-state simulations used in this study, but the fact that at least 60% of the saturated thickness at one nested-well location contained water recharged more than 9000 (^{14}C) years B.P. indicates recharge rates during the Early Holocene were larger than those in the Late Holocene. Additional radiocarbon ages are needed to further evaluate the temporal variability in recharge rates in southwestern Kansas during the Holocene.

On average, recent recharge under irrigated fields contained more NO_3 than paleorecharge (885 versus 193 μM). Values of δ ^{15}N[NO_3] indicate that NO_3 in paleorecharge was derived primarily from soil N and was similar to NO_3 currently present in the unsaturated zone in undisturbed areas. In contrast, δ ^{15}N[NO_3] values in

recent recharge beneath irrigated areas indicate varying proportions of fertilizer, manure, and soil N sources. These data indicate that the development of irrigated agriculture in the region has increased the flux of NO_3 to the aquifer. This finding is important because the aquifer has a limited natural remediation capacity for NO_3, as indicated by the slow denitrification rates ($5 \pm 2 \times 10^{-3}$ μmol N L^{-1} a^{-1}) estimated from the dated Holocene ground waters.

Acknowledgements

This study was part of the US Geological Survey's National Water-Quality Assessment (NAWQA) Program, High Plains Regional Ground-Water study. Thomas Bullen (USGS, Menlo Park, CA) provided the B and Sr isotope analyses. George Breit (USGS, Denver, CO) provided the X-ray diffraction analyses and mineral separates for isotope analysis. Craig Johnson (USGS, Denver, CO) provided the S isotope analyses on anhydrite and gypsum. Lawrence Skelton (Kansas Geological Survey, Wichita, KS) provided cuttings from oil and gas wells in the study area. The manuscript was improved by reviews from Brian Katz (USGS, Tallahassee, FL), Yousif Kharaka (USGS, Menlo Park, CA), Niel Plummer (USGS, Reston, VA), Margaret Townsend (Kansas Geological Survey, Lawrence, KS), and an anonymous journal reviewer. Use of product names are for identification purposes only and do not constitute an endorsement by the US Geological Survey.

References

Aeschbach-Hertig, W., Peeters, F., Beyerle, U., Kipfer, R., 2000. Paleotemperature reconstruction from noble gases in ground water taking into account equilibration with trapped air. Nature 405, 1040–1044.

Aeschbach-Hertig, W., Stute, M., Clark, J.F., Reuter, R.F., Schlosser, P., 2002. A paleotemperature record derived from dissolved noble gases in groundwater of the Aquia aquifer (Maryland, USA). Geochim. Cosmochim. Acta 66, 797–817.

Amberger, A., Schmidt, H.-L., 1987. Natürliche isotopengehalte von nitrat als indikatoren für dessen herkunft. Geochim. Cosmochim. Acta 51, 2699–2705.

American Society For Testing And Materials, 1992. Standard test methods for total and dissolved carbon dioxide in water. ASTM D513-92.

American Society For Testing And Materials, 1993. Standard test methods for instrumental determination of carbon, hydrogen, and nitrogen in laboratory samples of coal and coke. ASTM D5373-93.

Andrews, J.N., Lee, D.J., 1979. Inert gases in ground water from the Bunter Sandstone of England as indicators of age and paleoclimatic trends. J. Hydrol. 41, 233–252.

Aravena, R., Robertson, W.D., 1998. Use of multiple isotope tracers to evaluate denitrification in ground water: study of nitrate from a large-flux system plume. Ground Water 36, 975–982.

Back, W., Hanshaw, B.B., Plummer, L.N., Rahn, P.R., Rightmire, C.T., Rubin, M., 1983. Process and rate of dedolomitization: mass transfer and ^{14}C dating in a regional carbonate aquifer. Geol. Soc. Am. Bull. 94, 1415–1429.

Bard, E., Arnold, M., Fairbanks, R.G., Hamelin, B., 1993. ^{230}Th–^{234}U and ^{14}C ages obtained by mass spectrometry on corals. Radiocarbon 35, 191–199.

Ballentine, C.J., Sherwood-Lollar, B., 2002. Regional groundwater focusing of nitrogen and noble gases into the Hugoton-Panhandle giant gas field, USA. Geochim. Cosmochim. Acta 66, 2483–2497.

Bethke, C.M., Johnson, T.M., 2002. Ground-water age. Ground Water 40, 337–339.

Böhlke, J.K., Coplen, T.B., 1995. Interlaboratory comparison of reference materials for nitrogen-isotope-ratio measurements. In: Reference and Intercomparison Materials for Stable Isotopes of Light Elements. International Atomic Energy Agency, IAEA-TECDOC-825, pp. 51–66.

Böhlke, J.K., Denver, J.M., 1995. Combined use of groundwater dating, chemical, and isotopic analyses to resolve the history and fate of nitrate contamination in two agricultural watersheds, Atlantic Coastal Plain, Maryland. Water Resourc. Res. 31, 2319–2339.

Böhlke, J.K., Wanty, R., Tuttle, M., Delin, G., Landon, M., 2002. Denitrification in the recharge area and discharge area of a transient agricultural nitrate plume in a glacial outwash sand aquifer, Minnesota. Water Resourc. Res. 38, 10.1–10.26.

Böhlke, J.K., Mroczkowski, S.J., Coplen, T.B., 2003. Oxygen isotopes in nitrate: new reference materials for ^{18}O:^{17}O:^{16}O measurements and observations on nitrate-water equilibration. Rapid Commun. Mass Spectrom. 17, 1835–1846.

Boss International, 1997. GMS: Groundwater Modeling System user's manual. Madison, Wisc.

Böttcher, J., Strebel, O., Voerkelius, S., Schmidt, H.-L., 1990. Using isotope fractionation of nitrate-nitrogen and nitrate-oxygen for evaluation of microbial denitrification in a sandy aquifer. J. Hydrol. 114, 413–424.

Breit, G.N., Rice, C., Esposito, K., Schlottmann, J.L., 1990. Mineralogy and petrography of Permian rocks in the central Oklahoma aquifer. US Geol. Surv. Open File Rep. 90-678.

Bruce, B.W., Becker, M.F., Pope, L.M., Gurdak, J.J., 2003, Ground-water quality beneath irrigated agriculture in the central High Plains aquifer, 1999-2000. US Geol. Surv. Water Resour.-Invest. Rep. 03-4219.

Burke, W.H., Denison, R.E., Hetherington, E.A., Koepnick, R.B., Nelson, H.F., Otto, J.B., 1982. Variations of seawater $^{87}Sr/^{86}Sr$ throughout Phanerozoic time. Geology 10, 516–519.

Busby, J.F., Plummer, L.N., Lee, R.W., Hanshaw, B.B., 1991. Geochemical evolution of water in the Madison aquifer in parts of Montana, South Dakota, and Wyoming. US Geol. Surv. Prof. Pap. 1273-F.

Busenberg, E., Weeks, E.P., Plummer, L.N., Bartholomay, R.C., 1993. Age dating ground water by use of chlorofluorocarbons (CCl_3F and CCl_2F_2) and distribution of chlorofluorocarbons in the unsaturated zone, Snake River

Plain aquifer, Idaho National Engineering Laboratory, Idaho, USA. US Geol. Surv. Water Resourc. Invest. Rep. 93-4054.

Carmody, R.W., Plummer, L.N., Busenberg, E., Coplen, T.B., 1997. Methods for collection of dissolved sulfate and sulfide and analysis of their sulfur isotopic composition. US Geol. Surv. Open File Rep. 97-234.

Casciotti, K.L., Sigman, D.M., Hastings, M., Böhlke, J.K., Hilkert, A., 2002. Measurement of the oxygen isotopic composition of nitrate in seawater and freshwater using the denitrifier method. Anal. Chem. 74, 4905–4912.

Castro, M.C., Stute, M., Schlosser, P., 2000. Comparison of ^{4}He and ^{14}C ages in simple aquifer systems: implications for groundwater flow and chronologies. Appl. Geochem. 15, 1137–1167.

Cederstrand, J.R., and M.F. Becker, 1999. Digital map of predevelopment water levels for the High Plains aquifer in parts of Colorado, Kansas, Nebraska, New Mexico, Oklahoma, South Dakota, Texas, and Wyoming. US Geol. Surv. Open-File Rep. 99-264.

Clark, J.F., Davisson, M.L., Hudson, G.B., Macfarlane, P.A., 1998. Noble gases, stable isotopes, and radiocarbon as tracers of flow in the Dakota aquifer, Colorado and Kansas. J. Hydrol. 211, 151–167.

Coplen, T.B., 1988. Normalization of oxygen and hydrogen isotope data. Chem. Geol. 72, 293–297.

Coplen, T.B., Wildman, J.D., Chen, J., 1991. Improvements in the gaseous hydrogen-water equilibration technique for hydrogen isotope ratio analysis. Anal. Chem. 63, 910–912.

Craig, H., 1961. Isotopic variations in natural waters. Science 133, 1702–1703.

Darling, W.G., Edmunds, W.M., Smedley, P.L., 1997. Isotopic evidence for paleowater in the British Isles. Appl. Geochem. 12, 813–829.

Deines, P., 1980. The isotopic composition of reduced organic carbon. In: Fritz, P., Fontes, J.C. (Eds.), Handbook of Environmental Isotope Geochemistry, vol. 1. The Terrestrial Environment, Elsevier, Amsterdam, pp. 407–433.

Delwiche, C.C., Steyn, P.L., 1970. Nitrogen isotope fractionation in soils and microbial reactions. Environ. Sci. Technol. 4, 929–935.

Denison, R.E., Kirkland, D.W., Evans, R., 1998. Using strontium isotopes to determine the age and origin of gypsum and anhydrite beds. J. Geol. 106, 1–17.

Dutton, A.R., 1995. Ground water isotopic evidence for paleorecharge in US High Plains aquifers. Quater. Res. 43, 221–231.

Edmunds, W.M., Smedley, P.L., 2000. Residence time indicators in ground water: the East Midlands Triassic sandstone aquifer. Appl. Geochem. 15, 737–752.

Epstein, S., Mayeda, T., 1953. Variation of O-18 content of water from natural sources. Geochim. Cosmochim. Acta 4, 213–224.

Fishman, M.J., Friedman, L.C., 1989. Methods for the determination of inorganic substances in water and fluvial sediments. US Geol. Surv. Techn. Water Resourc. Invest. (Book 5, Chapter A1).

Frette, L., Gejlsbjerg, B., Westermann, P., 1997. Aerobic denitrifiers isolated from an alternating activated sludge system. FEMS Microbiol. Ecol. 24, 363–370.

Fryar, A.E., Mullican, W.F., Macko, S.A., 2001. Groundwater recharge and chemical evolution in the southern High Plains of Texas, USA. Hydrogeol. J. 9, 522–542.

Gustavson, T.C., Finley, R.J., McGillis, K.A., 1980. Regional dissolution of Permian salt in the Anadarko, Dalhart, and Palo Duro Basins of the Texas Panhandle. Texas Bureau of Econ. Geol. Rep. Invest. 106.

Gutentag, E.D., Lobmeyer, D.H., Slagle, S.E., 1981. Geohydrology of southwestern Kansas, Kansas Geol. Surv. Irrigation Ser. 7.

Gutentag, E.D., Heimes, F.J., Krothe, N.C., Luckey, R.R., Weeks, J.B., 1984. Geohydrology of the High Plains aquifer in parts of Colorado, Kansas, Nebraska, New Mexico, Oklahoma, South Dakota, Texas, and Wyoming. US Geol. Surv. Prof. Pap. 1400-B.

Harbaugh, A.W., McDonald, M.G., 1996. User's documentation for MODFLOW-96, an update to the US Geological Survey modular finite-difference ground-water flow model. US Geol. Surv. Open File Rep. 96-485.

Herbel, M.J., Spalding, R.F., 1993. Vadose zone fertilizer-derived nitrate and δ ^{15}N extracts. Ground Water 31, 376–382.

High Plains Regional Climate Center, accessed on the World Wide Web at: http://hpccsun.unl.edu/ on 1/29/02.

Hübner, H., 1986. Isotope effects of nitrogen in the soil and biosphere. In: Fritz, P., Fontes, J.C. (Eds.), Handbook of Environmental Isotope Geochemistry, Elsevier, Amsterdam, vol. 2, pp. 361–425.

Jenden, P.D., Newell, K.D., Kaplan, I.R., Watney, W.L., 1988a. Composition and stable-isotope geochemistry of natural gases from Kansas, Midcontinent, USA. Chem. Geol. 71, 117–147.

Jenden, P.D., Kaplan, I.R., Poreda, R.J., Craig, H., 1988b. Origin of nitrogen-rich natural gases in the California Great Valley; evidence from helium, carbon, and nitrogen isotope ratios. Geochim. Cosmochim. Acta 52, 851–861.

Jones, O.R., Schneider, A.D., 1969. Determining specific yield of the Ogallala aquifer by the neutron method. Water Resourc. Res. 5, 1267–1272.

Jorgensen, D.G., Helgesen, J.O., Imes, J.L., 1993. Regional aquifers in Kansas, Nebraska, and parts of Arkansas, Colorado, Missouri, New Mexico, Oklahoma, South Dakota, Texas, and Wyoming—Geohydrologic Framework. US Geol. Surv. Prof. Pap. 1414-B.

Klots, C.E., Benson, B.B., 1963. Isotope effect in the solution of oxygen and nitrogen in distilled water. J. Chem. Phys. 38, 890–892.

Korom, S.F., 1992. Natural denitrification in the saturated zone: a review. Water Resourc. Res. 28, 1657–1668.

Koterba, M.T., Wilde, F.D., Lapham, W.W., 1995. Groundwater data-collection protocols and procedures for the National Water-Quality Assessment Program–Collection and documentation of water-quality samples and related data. US Geol. Surv. Open File Rep. 95-399.

Krothe, N.C., Oliver, J.W., 1982. Sulfur isotopic composition and water chemistry in water from the High Plains aquifer, Oklahoma Panhandle and southwestern Kansas. US Geol. Surv. Water Resourc. Invest. Rep. 82-12.

Lindau, C.W., Spalding, R.F., 1984. Major procedural discrepancies in soil extracted nitrate levels and nitrogen isotope values. Ground Water 22, 273–278.

Luckey, R.R., Gutentag, E.D., Heimes, F.J., Weeks, J.B., 1986. Digital simulation of ground-water flow in the High Plains aquifer in parts of Colorado, Kansas, Nebraska, New Mexico, Oklahoma, South Dakota, Texas, and Wyoming. US Geol. Surv. Prof. Pap. 1400-D.

Luckey, R.R., Becker, M.F., 1998. Estimated predevelopment discharge to streams from the High Plains aquifer in northwestern Oklahoma, southwestern Kansas, and northwestern Texas. US Geol. Survey Water Resourc. Invest. Rep. 97-4287.

Luckey, R.R., Becker, M.F., 1999. Hydrogeology, water use, and simulation of flow in the High Plains aquifer in northwestern Oklahoma, southeastern Colorado, southwestern Kansas, northeastern New Mexico, and northwestern Texas. US Geol. Surv. Water Resourc. Invest. Rep. 99-4104.

Ludin, A., Weppernig, R., Bönisch, G., Schlosser, P., 1998. Mass spectrometric measurement of helium isotopes and tritium. Lamont-Doherty Technical Report 98-06. Available from: <http://www.ldeo.columbia.edu/~etg/ms_ms/Ludin_et_al_MS_Paper.html>.

Macfarlane, P.A., Combes, J., Turbek, S., Kirshen, D., 1993. Shallow subsurface bedrock geology and hydrostratigraphy of southwestern Kansas. Kansas Geol. Surv. Open File Rep. 93-1a.

Mariotti, A., Landreau, A., Simon, B., 1988. ^{15}N isotope biogeochemistry and natural denitrification process in ground water: application to the chalk aquifer of northern France. Geochim. Cosmochim. Acta 52, 1869–1878.

Mazaud, A., Laj, C., Bard, E., Arnold, M., Tric, E., 1991. Geomagnetic field control of ^{14}C production over the last 80 ky: implications for the radiocarbon time scale. Geophys. Res. Lett. 18, 1885–1888.

McGuire, V.L., Sharpe, J.B., 1997. Water-level changes in the High Plains aquifer–predevelopment to 1995. US Geol. Surv. Water Resourc. Invest. Rep. 97-4081, 2 maps.

McMahon, P.B., 2001. Vertical gradients in water chemistry in the central High Plains aquifer, southwestern Kansas and Oklahoma Panhandle, 1999. US Geol. Surv. Water Resourc. Invest. Rep. 01-4028.

McMahon, P.B., Dennehy, K.F., Michel, R.L., Sophocleous, M.A., Ellett, K.M., Hurlbut, D.B., 2003. Water movement through thick unsaturated zones overlying the central High Plains aquifer, southwestern Kansas, 2000-2001, US Geol. Surv. Water Resourc. Invest. Rep. 03-4171, 32 pp.

Meyer, W.R., Gutentag, E.D., Lobmeyer, D.H., 1970. Geohydrology of Finney County, southwestern Kansas. US Geol. Surv. Water Supply Pap. 1891.

Olson, C.G., Nettleton, W.D., Porter, D.A., Brasher, B.R., 1997. Middle Holocene aeolian activity on the High Plains of west-central Kansas. The Holocene 7, 255–261.

Olson, C.G., Porter, D.A., 2002. Isotopic and geomorphic evidence for Holocene climate, southwestern Kansas. Quatern. Int. 87, 29–44.

Parkhurst, D.L., Christenson, S., Breit, G.N., 1992. Groundwater-quality assessment of the central Oklahoma aquifer, Oklahoma: geochemical and geohydrologic investigations. US Geol. Surv. Open File Rep. 92-642.

Phillips, F.M., Peeters, L.A., Tansey, M.K., Davis, S.N., 1986. Paleoclimate inferences from an isotopic investigation of groundwater in the central San Juan Basin, New Mexico. Quatern. Res. 26, 179–193.

Plummer, L.N., Sprinkle, C.L., 2001. Radiocarbon dating of dissolved inorganic carbon in groundwater from confined parts of the Upper Floridan aquifer, Florida, USA. Hydrogeol. J. 9, 127–150.

Plummer, L.N., Parkhurst, D.L., Fleming, G.W., Dunkle, S.A., 1988. A computer program incorporating Pitzer's equations for calculation of geochemical reactions in brines. US Geol. Surv. Water Resourc. Invest. Rep. 88-4153.

Plummer, L.N., Busby, J.F., Lee, R.W., Hanshaw, B.B., 1990. Geochemical modeling of the Madison aquifer in parts of Montana, Wyoming, and South Dakota. Water Resources Res. 26, 1981–2014.

Plummer, L.N., 1993. Stable isotope enrichment in paleowaters of the southeast Atlantic Coastal Plain, United States. Science 262, 2016–2020.

Plummer, L.N., Prestemon, E.C., Parkhurst, D.L., 1994. An interactive code (NETPATH) for modeling NET geochemical reactions along a flow PATH, version 2.0. US Geol. Surv. Water Resourc. Invest. Rep. 94-4169, 130 pp.

Pollock, D.W., 1994. User's guide for MODPATH/MODPATH-PLOT, version 3: A particle tracking post-processing package for MODFLOW, the US Geological Survey finite-difference ground-water flow model. US Geol. Surv. Open File Rep. 94-464, pp.

Sanford, W.E., 1997. Correcting for diffusion in carbon-14 dating of ground water. Ground Water 35, 357–361.

Sigman, D.M., Casciotti, K.L., Andreani, M., Barford, C., Galanter, M., Böhlke, J.K., 2001. A bacterial method for the nitrogen isotopic analysis of nitrate in seawater and freshwater. Anal. Chem. 73, 4145–4153.

Skerman, V.B.D., MacRae, I.C., 1957. The influence of oxygen availability on the degree of nitrate reduction by Pseudomonas denitrificans. Can. J. Microbiol. 3, 505–530.

Smith, H.T.U., 1940. Geological studies in southwestern Kansas. Kansas Geol. Surv. Bull. 34.

Solley, W.B., Pierce, R.R., Perlman, H.A., 1993, Estimated Use of Water in the United States in 1990. US Geological Survey Circular 1081, available on the World Wide Web at http://water.usgs.gov/watuse/wucircular2.html.

Stute, M., Schlosser, P., 1993. Principles and applications of the noble gas paleothermometer. In: Swart, P.K., Lohmann, K.C., McKenzie, J., Savin, S. (Eds.), Climate change in continental isotope records. In: Geophys Monograph, vol. 78, pp. 89–100.

Stute, M., Clark, J.F., Schlosser, P., Broecker, W.S., 1995. A 30,000 yr continental paleotemperature record derived from noble gases dissolved in groundwater from the San Juan Basin, New Mexico. Quatern. Res. 43, 209–220.

Stute, M., Schlosser, P., Clark, J.F., Broecker, W.S., 1992. Paleotemperatures in the southwestern United States derived from noble gases in ground water. Science 256, 1000–1003.

Thatcher, L.L., 1962. The distribution of tritium fallout in precipitation over North America. Bull. Int. Assoc. Sci. Hydrol. 7, 48–58.

Theis, C.V., 1937. Amount of ground-water recharge in the southern High Plains. Trans. Am. Geophys. Union 18, 564–568.

Vogel, J.C., Talma, A.S., Heaton, T.H.E., 1981. Gaseous nitrogen as evidence for denitrification in ground water. J. Hydrol. 50, 191–200.

Walters, L.J., Claypool, G.E., Chouquette, P.W., 1972. Reaction rates and $\delta\ ^{18}O$ variation for the carbonate-phosphoric acid preparation method. Geochim. Cosmochim. Acta 36, 129–140.

Weiss, R.F., 1970. The solubility of nitrogen, oxygen, and argon in water and seawater. Deep-Sea Res. 17, 721–735.

Weiss, R.F., 1971. Solubility of helium and neon in water and seawater. J. Chem. Eng. Data 16, 235–241.

Wershaw, R.L., Fishman, M.J., Grabbe, R.R., Lowe, L.E., 1987. Methods for the determination of organic substances in water and fluvial sediments. US Geological Survey Techniques of Water Resources Investigations (Book 5, Chapter A3).

Whittemore, D.O., 1984. Geochemical identification of the source of salinity in groundwaters of southeastern Seward County. Kansas Geol. Surv. Open File Rep., 84-3.

Whittemore, D.O., 1993. Ground-water geochemistry in the mineral intrusion area of Groundwater Management District No. 5, south-central Kansas. Kansas Geol. Surv. Open File Rep., 93-2, 107 pp.

Whittemore, D.O., Macfarlane, P.A., Doveton, J.H., Butler, J.J., Tyan-ming, C., Bassler, R., Smith, M., Mitchell, J., Wade, A., 1993. The Dakota Aquifer Program Annual Report, FY92. Kansas Geol. Surv. Open File Rep., 93-1, 170 pp.